Methylidyne XC≡MX₃ (M = Cr, Mo, W; X = H, F, Cl) Diagnostic C−H and C−X Stretching Absorptions and Methylidene CH₂=MX₂ Analogues

Jonathan T. Lyon,[†] Han-Gook Cho,[‡] and Lester Andrews*

Department of Chemistry, University of Virginia, Charlottesville, Virginia 22904-4319

Received July 10, 2007

Laser-ablated Cr, Mo, and W atoms react with di-, tri-, and tetrahalomethanes to form XC≡MX₃ (M = Mo, W; X = H, F, Cl) methylidyne molecules as major products. Dihalomethanes also give a minor yield of CH₂=MX₂ methylidenes. The electronic state and bonding changes in the CH₂=CrCl₂, CH₂=CrFCl, and CH₂−CrF₂ methylidene series, but the Mo and W counterparts are calculated to be triplet state CH₂=MX₂ molecules. Identifications of these new carbon−metal multiple bond species are made through isotopic substitution (D, ^{13}C) and isotopic frequency calculations using density functional theory. The HC≡MX₃ molecules exhibit C−H stretching frequencies in the 3030−3090 cm^{-1} region and C≡M stretching frequencies in the 1007−980 cm^{-1} range, which vary slightly with the carbon hybridization as determined by the substituents employed here. The XC≡MX₃ molecules show very high C−X stretching frequencies in the 1540−1520 cm^{-1} region for X = F and 1300−1230 cm^{-1} for X = Cl due to strong bonds and the antisymmetric nature of the X−C−M vibrational mode.

Introduction

Compounds containing carbon−transition metal triple bonds have been investigated extensively for their varied chemistry and catalytic metathesis of alkynes.[1−4] These organometallic complexes necessarily contain the C≡M bond, but most also contain a variety of substituents and ligands that affect the vibrational frequencies that could characterize the backbone of these interesting molecules.[5−7] A limited number of such complexes contain the simple M≡C−H moiety, and even fewer incorporate the halogen substituent as M≡C−X (M = transition metal).[1−5] Although the C−H vibrational characteristics are difficult to investigate due to very low infrared intensity and interference from other hydrogen stretching absorptions,[6,7] the C−X stretching bands are very intense and appear in a clean region of the spectrum. Both modes can be used as a probe to study the hybridization at carbon in the multiple bond. Accordingly, we have prepared the doublet ground-state HC≡ReH₃ complex in solid argon for observation of the C−H stretching mode at 3101.8 cm^{-1}, and density functional calculations show

45.6% s-character in the bond and distortion to C_s symmetry.[8] This fundamentally important simple methylidyne complex can be investigated by high level theoretical calculations to understand the unique bonding and structure around the Re center including Jahn−Teller distortion and symmetry reduction.

The (HC≡W)(PMe₃)₄Cl complex is a unique host for the methylidyne ligand, and detailed vibrational spectroscopic investigations of this species have been performed to explore the nature of the metal−carbon triple bond.[6,7] Both the C−H and the C≡W bonds are deduced to be slightly longer and the C≡W stretching frequency about 100 cm^{-1} lower than that found in the laser excitation spectrum of H−C≡W formed in the reaction of laser-ablated W and methane in the gas phase.[9]

Recently, a new class of electron-deficient triplet state methyidyne complexes XC÷MX₃ has been prepared from group 4 atom reactions with CX₄ (X = F and Cl) molecules. Chlorofluoromethane reactions were also investigated, and both possible structural isomers were observed. The thermochemical driving force for complete α-F transfer dominated these reactions and provided a very high diagnostic C−F stretching mode in the 1460−1410 cm^{-1} region.[10−12] Additional work with methylene halides and haloforms also revealed extensive α-halogen transfer reactions.[13]

Group 6 metals form the backbone for high-oxidation state alkylidene (R₁R₂C=M) and alkylidyne (RC≡M) complexes; however, there are relatively few examples of chromium alkylidene and alkylidyne complexes.[3a] Chromium alkylidynes

* Corresponding author. E-mail: lsa@virginia.edu.
† Present address: Fritz-Haber-Institut der Max-Planck-Gesellschaft, Faradayweg 4-6, D-14195 Berlin, Germany.
‡ Visiting scientist: Department of Chemistry, University of Incheon, 177 Dohwa-dong, Nam-ku, Incheon 402-749, South Korea.
(1) Fischer, E. O.; Kreis, G.; Kreiter, C. G.; Müller, J.; Huttner, G.; Lorenz, H. *Angew. Chem., Int. Ed. Engl.* **1973**, *12*, 564.
(2) McLain, S. J.; Wood, C. D.; Messerle, L. W.; Schrock, R. R.; Hollander, F. J.; Youngs, W. J.; Churchill, M. R. *J. Am. Chem. Soc.* **1978**, *100*, 5962 (carbyne synthesis).
(3) (a) Schrock, R. R. *Chem. Rev.* **2002**, *102*, 145. (b) Herndon, J. W. *Coord. Chem. Rev.* **2004**, *248*, 3. (c) Herndon, J. W. *Coord. Chem. Rev.* **2005**, *24*, 999. (d) Herndon, J. W. *Coord. Chem. Rev.* **2006**, *250*, 1889.
(4) Nugent, W. A.; Mayer, J. M. *Metal-Ligand Multiple Bonds*; John Wiley and Sons: New York, 1988.
(5) Foulet-Fonseca, G. P.; Jouan, M.; Dao, N. Q.; Fischer, H.; Schmid, J.; Fischer, E. O. *Spectrochim. Acta* **1990**, *46A*, 339.
(6) Manna, J.; Kuk, R. J.; Dallinger, R. F.; Hopkins, M. D. *J. Am. Chem. Soc.* **1994**, *116*, 9793 ((H−C≡W)(PMe₃)₄Cl).
(7) Manna, J.; Dallinger, R. F.; Miskowski, V. M.; Hopkins, M. D. *J. Phys. Chem. B* **2000**, *104*, 10928 ((H−C≡W)(PMe₃)₄Cl).

(8) Cho, H.-G.; Andrews, L. *Organometallics* **2007**, *26*, 4098 (HC≡ReH₃ complex).
(9) Barnes, D.; Gillett, D. A.; Merer, A. J.; Metha, G. F. *J. Chem. Phys.* **1996**, *105*, 6168 (W≡C−H emission spectrum).
(10) Lyon, J. T.; Andrews, L. *Inorg. Chem.* **2006**, *45*, 9858 (Ti + CF₄).
(11) Lyon, J. T.; Andrews, L. *Organometallics* **2007**, *26*, 2519 (Gr 4 + CX₄, CF₂Cl₂).
(12) Lyon, J. T.; Andrews, L. *Organometallics* **2007**, *26*, 4152 (Gr 4 + CF₃X).
(13) (a) Lyon, J. T.; Andrews, L. *Organometallics* **2007**, *26*, 332 (Gr 4 + CH₂Cl₂, CHCl₃). (b) Lyon, J. T.; Andrews, L. *Inorg. Chem.* **2007**, *46*, 4799 (Gr 4 + CH₂F₂, CHF₃).

have been prepared with dialkylamino substituents, but these species are not stable above −50 °C. The isocyanide or trimethyl phosphate complexes are more stable.[3a,14] X-ray analysis has found C≡Cr bond lengths in the 1.74 Å range. Chromium is more thermally accessible than Mo and W, and the CH_2=Cr complex has been investigated.[15]

Methylidyne complexes have appeared as major products in Mo and W atom reactions with methane and methyl halides,[16−21] and similar HC≡MX_3 methylidyne compounds are expected to be prominent in group 6 metal reactions with methylene halides, haloforms, and CX_4 precursors in particular because this group dominates the alkylidyne complex literature.[3]

Experimental and Computational Methods

Laser ablated Cr, Mo, and W atoms (Johnson-Matthey) were reacted with CH_2X_2, CHX_3, CX_4, CF_2Cl_2, CF_3Cl (DuPont), $^{13}CF_3$-Cl, $^{13}CF_2Cl_2$ (prepared),[22,23] CD_2Cl_2, $CDCl_3$, $^{13}CH_2Cl_2$, $^{13}CHCl_3$, and $^{13}CCl_4$ (Cambridge Isotope) in excess argon during condensation at 8 K using a closed-cycle refrigerator (Air Products HC-2). These methods have been described in detail elsewhere.[24,25] Reagent gas mixtures were typically 0.5−1% in argon. After reaction, infrared spectra were recorded at a resolution of 0.5 cm^{-1} using a Nicolet 550 spectrometer with an Hg−Cd−Te B range detector. Samples were later irradiated for 10 min periods by a mercury arc lamp (175 W) with the globe removed using a combination of optical filters, and then samples were annealed to allow reagent diffusion and further reaction.

Complementary density functional theory (DFT) calculations were carried out using the Gaussian 98 package,[26] the hybrid B3LYP density functional,[27] the 6-311++G(2d,p) basis sets for C, H, F, and Cl,[28] and the SDD pseudopotential and basis set[29] for the metals to provide a consistent set of vibrational frequencies for the reaction products. Different spin states were computed to locate the ground-state product molecule. Additional BPW91 calculations

Figure 1. Infrared spectra in the 2970−2920 and 590−460 cm^{-1} regions for the Cr atom and CH_2Cl_2 reaction products in excess argon at 8 K. (a) Cr + 0.5% CH_2Cl_2 in argon co-deposited for 1 h. (b) After irradiation (λ > 220 nm). (c) Cr + 0.5% $^{13}CH_2Cl_2$ in argon co-deposited for 1 h. (d) After irradiation (λ > 220 nm). (e) Cr + 0.5% CD_2Cl_2 in argon. (f) After irradiation (λ > 220 nm). The lable **m** denotes the methylidene complex absorptions, **i** denotes the insertion product, and vertical lines indicate chlorine isotopic splittings.

were performed for selected reaction products to support the B3LYP results. Geometries were fully relaxed during optimization, and the optimized geometry was confirmed by vibrational analysis. All of the vibrational frequencies were calculated analytically with zero-point energy included in the calculation of reaction energies. Natural bond order (NBO)[26,30]analysis was also done to explore the bonding in new methylidyne molecules.

Results and Discussion

The reaction products of Cr, Mo, and W atoms with polyhalomethane precursors will be characterized by matrix infrared spectra and density functional theory calculations. These experiments also reveal absorptions due to precursor fragment and parent anion reactive species that have been reported previously.[22,31]

Cr + CH_2X_2. Infrared spectra of the reaction product from laser-ablated Cr and CH_2Cl_2 are illustrated in Figure 1. Three sets of product absorptions with different behaviors on ultraviolet irradiation were observed. Weak new absorptions at 575.7 and 561.0 cm^{-1} with carbon-12 and -13 samples (labeled **i**) were destroyed by >220 nm irradiation. A new band at 2937.2 cm^{-1} and a strong partially resolved triplet at 513.3, 511.2, 508.0 cm^{-1} (labeled **m**) were not affected by >290 nm irradiation, but they doubled on >220 nm irradiation. A new weaker 487.5 cm^{-1} band with a 483.3 cm^{-1} shoulder also appeared on >220 nm irradiation. The associated **m** pair was shifted slightly with carbon-13, as given in Table 1, but the 487.5 cm^{-1} band was not shifted. The weak high-frequency band was not observed with CD_2Cl_2, but a new band was observed at 545.1 cm^{-1}, and the triplet was better resolved at 506.4, 503.7, and 500.8 cm^{-1}.

(14) (a) Flippou, A. C.; Lungwitz, B.; Wanninger, K. M. A.; Herdtweck, E. *Angew. Chem., Int. Ed. Engl.* **1995**, *34*, 924. (b) Flippou, A. C.; Fischer, E. O. *J. Organomet. Chem.* **1990**, *382*, 143.

(15) Billups, W. E.; Chang, S.-C.; Hauge, R. H.; Margrave, J. L. *Inorg. Chem.* **1993**, *32*, 1529.

(16) Cho, H.-G.; Andrews, L. *Chem.-Eur. J.* **2005**, *11*, 5017 (Mo + CH_3F).

(17) Cho, H.-G.; Andrews, L. *J. Am. Chem. Soc.* **2005**, *127*, 8226 (Mo + CH_4).

(18) Cho, H.-G.; Andrews, L. *Organometallics* **2005**, *24*, 5678 (Cr and W + CH_3F).

(19) Cho, H.-G.; Andrews, L.; Marsden, C. *Inorg. Chem.* **2005**, *44*, 7634 (W + CH_4).

(20) Cho, H.-G.; Andrews, L. *J. Phys. Chem. A* **2006**, *110*, 13151 (Mo, W + CH_3X).

(21) Andrews, L.; Cho, H.-G. *Organometallics* **2006**, *25*, 4040 and references therein (review article).

(22) Prochaska, F. T.; Andrews, L. *J. Chem. Phys.* **1978**, *68*, 5577.

(23) (a) Prochaska, F. T.; Andrews, L. *J. Am. Chem. Soc.* **1978**, *100*, 2102. (b) Andrews, L.; Willner, H.; Prochaska, F. T. *J. Fluorine Chem.* **1979**, *13*, 273.

(24) Andrews, L.; Citra, A. *Chem. Rev.* **2002**, *102*, 885 and references therein.

(25) Andrews, L. *Chem. Soc. Rev.* **2004**, *33*, 123 and references therein.

(26) Frisch, M. J.; Trucks, G. W.; Schlegel, H. B.; Scuseria, G. E.; Robb, M. A.; Cheeseman, J. R.; Zakrzewski, V. G.; Montgomery, J. A., Jr.; Stratmann, R. E.; Burant, J. C.; Dapprich, S.; Millam, J. M.; Daniels, A. D.; Kudin, K. N.; Strain, M. C.; Farkas, O.; Tomasi, J.; Barone, V.; Cossi, M.; Cammi, R.; Mennucci, B.; Pomelli, C.; Adamo, C.; Clifford, S.; Ochterski, J.; Petersson, G. A.; Ayala, P. Y.; Cui, Q.; Morokuma, K.; Rega, N.; Salvador, P.; Dannenberg, J. J.; Malick, D. K.; Rabuck, A. D.; Raghavachari, K.; Foresman, J. B.; Cioslowski, J.; Ortiz, J. V.; Baboul, A. G.; Stefanov, B. B.; Liu, G.; Liashenko, A.; Piskorz, P.; Komaromi, I.; Gomperts, R.; Martin, R. L.; Fox, D. J.; Keith, T.; Al-Laham, M. A.; Peng, C. Y.; Nanayakkara, A.; Challacombe, M.; Gill, P. M. W.; Johnson, B.; Chen, W.; Wong, M. W.; Andres, J. L.; Gonzalez, C.; Head-Gordon, M.; Replogle, E. S.; Pople, J. A. *Gaussian 98*, revision A.11.4; Gaussian, Inc.: Pittsburgh, PA, 2002.

(27) (a) Becke, A. D. *J. Chem. Phys.* **1993**, *98*, 5648. (b) Lee, C.; Yang, Y.; Parr, R. G. *Phys. Rev. B* **1988**, *37*, 785.
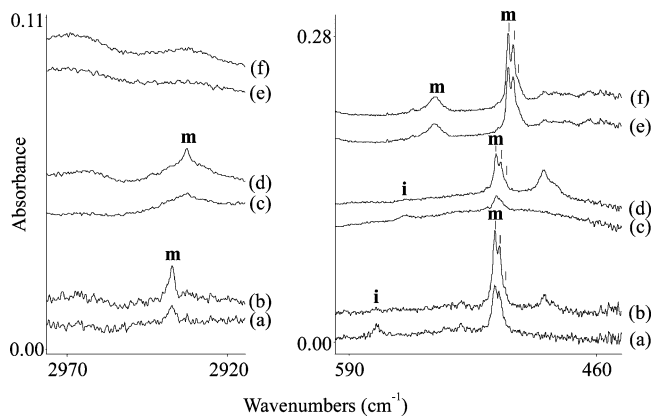
(28) Frisch, M. J.; Pople, J. A.; Binkley, J. S. *J. Chem. Phys.* **1984**, *80*, 3265.

(29) Andrae, D.; Haeussermann, U.; Dolg, M.; Stoll, H.; Preuss, H. *Theor. Chim. Acta* **1990**, *77*, 123.

(30) (a) Reed, A. E.; Weinstock, R. B.; Weinhold, F. *J. Chem. Phys.* **1985**, *83*, 735. (b) Reed, A. E.; Curtiss, L. A.; Weinhold, F. *Chem. Rev.* **1988**, *88*, 899.

(31) (a) Milligan, D. E.; Jacox, M. E.; McAuley, J. H.; Smith, C. E. *J. Mol. Spectrosc.* **1973**, *45*, 377. (b) Prochaska, F. T.; Andrews, L. *J. Phys. Chem.* **1978**, *82*, 1731. (c) Andrews, L.; Prochaska, F. T. *J. Phys. Chem.* **1979**, *83*, 824. (d) Andrews, L.; Prochaska, F. T. *J. Am. Chem. Soc.* **1979**, *101*, 1190. (Cl$^-$)(HCCl$_2$) (e) Maier, G.; Reisenauer, H. P.; Ju, J.; Hess, B. A.; Schaad, L. J. *Tetrahedron Lett.* **1989**, *30*, 4105.

Table 1. Observed and Calculated Fundamental Frequencies of $CH_2=CrCl_2$ in the Ground $^3A_2$ Electronic State with C_{2v} Symmetry[a]

approximate description	$CH_2=CrCl_2$			$^{13}CH_2=CrCl_2$			$CD_2=CrCl_2$		
	obs	calc	int	obs	calc	int	obs	calc	int
C−H str, b_2		3187.1	0		3174.3	0		2369.1	0
C−H str, a_1	2937.2	3074.4	2	2932.5	3069.5	2	not obs	2221.8	2
HCH bend, a_1		1303.7	1		1295.9	1		990.2	1
CH₂ wag, b_1	—[b]	700.0	62	—[b]	693.4	61	545.1	546.8	47
C=Cr str, a_1		602.2	41		586.4	40		562.2	32
Cr−Cl str, b_2	513.3[c]	534.3	81	512.8[c]	530.4	81	506.4[c]	498.5	117
CH₂ twist, a_2		438.7	43		436.7	42		377.0	21
Cr−Cl str, a_1		379.4	23		378.0	22		357.6	7

[a] Frequencies and intensities are in cm⁻¹ and km/mol. Four lower real frequencies are not listed. Observed in an argon matrix. Frequencies and intensities computed with B3LYP/6-311++G(2d,p) in harmonic approximation using the SDD core potential and basis set for Cr. $\langle s^2 \rangle$ values are 2.64 before and 2.07 after annihilation. Symmetry notations are based on the C_{2v} structure. [b] Band covered by precursor. [c] Frequency for ^{35}Cl isotope. Resolved chlorine isotopic bands at 511.2 and 508.0 cm⁻¹ for $CH_2=CrCl_2$ and at 503.7 and 500.8 cm⁻¹ for $CD_2=CrCl_2$.

The profile of the strong new band near 500 cm⁻¹ is nearly the 9/6/1 relative intensities expected for the vibration of two equivalent chlorine atoms. A diatomic Cr−Cl oscillator at this frequency would shift 8.3 cm⁻¹ from Cl-35 to Cl-37, and our maximum shift is measured as 5.6 cm⁻¹; however, the antisymmetric stretching mode of a $CrCl_2$ subunit with a 125° valence angle would shift 5.9 cm⁻¹, which is very close to what we observed. Hence, we can assign the triplet with confidence to the antisymmetric Cr−Cl stretching mode of a molecule containing a $CrCl_2$ subgroup. This finds support from the preparation of $CrCl_2$ itself through the reaction of chlorine gas and hot chromium metal, and its characterization by a chlorine isotopic triplet absorption at 493.5, 490.4, 487.3 cm⁻¹ in solid argon.[32]

The weak 2937.2 cm⁻¹ band shifts just 4.7 cm⁻¹ with carbon-13, which is about one-half of the shift for one uncoupled C−H bond vibration. Our calculation for $CH_2=CrCl_2$ predicts a 4.9 cm⁻¹ shift for the symmetric C−H and 12.8 cm⁻¹ for the antisymmetric C−H stretching mode where the average is about right for a single C−H vibration (10.7 cm⁻¹ for HC≡MoF₂Cl, for example). Hence, the small carbon-13 shift characterizes this motion as the symmetric stretching mode of a CH_2 subgroup, and the product is identified as the $CH_2=CrCl_2$ methylidene molecule. The CH_2 wagging mode is often difficult to calculate, and this mode predicted at 700 cm⁻¹ is probably covered by precursor absorption in this region; however, the CD_2 counterpart is observed at 545.1 cm⁻¹. Further support is found from comparison with the calculated frequencies for triplet $CH_2=CrCl_2$ listed in Table 1. The calculated frequencies are higher than the observed values by 4.7% and 4.1%, respectively, which is expected for the B3LYP density functional.[33] Finally, the strong diagnostic Cr−Cl stretching mode predicted for the 4 kcal/mol higher energy quintet single-bonded $CH_2−CrCl_2$ species at 468 cm⁻¹ is therefore not compatible with our strong observed 513.3 cm⁻¹ band.

The 487.5 cm⁻¹ band that appears on ultraviolet irradiation when $CH_2=CrCl_2$ increases cannot be identified with certainty, but it shows no C nor D isotopic shift and a chlorine profile similar to the nearby methylidene. The CrCl molecule has been observed in the gas phase, and its fundamental is 397 cm⁻¹.[34] The 487.5 cm⁻¹ photoproduct is likely to be due to a different matrix trapping site of isolated chromium dichloride, which is produced here under different conditions.

In addition, the weak 575.7 cm⁻¹ band correlates with the strongest absorption calculated for the chlorine bridge-bonded quintet $CH_2Cl−CrCl$ insertion product (Table S1) that is within our instrumental limit. The much stronger Cr−Cl stretching mode is calculated at 394.9 cm⁻¹ and cannot be observed here. The 14.7 cm⁻¹ carbon-13 shift observed for the 575.7 cm⁻¹ band is in agreement with the predicted 14.6 cm⁻¹ shift, which identifies this mode as the mostly C−Cr stretching mode of the insertion product first formed in the reaction (a pure diatomic C−Cr oscillator would shift 18.2 cm⁻¹).

The reaction proceeds first through the quintet $CH_2Cl−CrCl$ insertion product, which has a Cl bridged structure and is 66 kcal/mol lower in energy than the Cr and CH_2Cl_2 reagents. The triplet methylidene complex $CH_2=CrCl_2$ is 8 kcal/mol higher in energy. This methylidene was computed with different spin multiplicities, and the quintet ground-state 90° dihedral $CH_2−CrCl_2$ is 12 kcal/mol higher, the singlet coplanar $CH_2=CrCl_2$ is 49 kcal/mol higher, and the coplanar quintet structure is 68 kcal/mol higher in energy than the quintet insertion product. A singlet distorted methylidyne is also computed to be 49 kcal/mol higher than the insertion product, and such a higher energy species is unlikely to be formed and trapped here. The reaction to form the triplet $CH_2=CrCl_2$ methylidene is 58 kcal/mol exothermic.

$$Cr^* + CH_2Cl_2 \rightarrow CH_2Cl−CrCl^* \rightarrow CH_2=CrCl_2 \quad (1a)$$
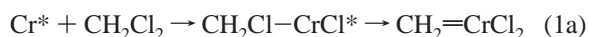
It is interesting that the reaction product energies are slightly different for methylene fluoride. The quintet insertion product $CH_2F−CrF$ is 47 kcal/mol lower in energy than the reactants, and the triplet methylidene is 9 kcal/mol higher, but the quintet methylidene is now 1.4 kcal/mol lower in energy than the first quintet insertion product. Hence, the most stable product for these reagents is the quintet methylidene, reaction 1b. Our infrared spectra, observed, and calculated frequencies that validate this conclusion are given in Figure S2 and Table S2. Because CrF_2 itself has been reported to absorb at 749 cm⁻¹ in solid argon,[35] the strong band we observed at 746.4 cm⁻¹ with matrix site splitting at 754.8 cm⁻¹ is appropriate for the strong antisymmetric Cr−F stretching mode in the $CH_2−CrF_2$ molecule.

$$Cr^* + CH_2F_2 \rightarrow CH_2F−CrF^* \rightarrow CH_2−CrF_2 \quad (1b)$$

These interesting differences between the dichloro- and difluoromethane products suggested experiments with CH_2FCl.

(32) Jacox, M. E.; Milligan, D. E. *J. Chem. Phys.* **1969**, *51*, 4143.

(33) (a) Scott, A. P.; Radom, L. *J. Phys. Chem.* **1996**, *100*, 16502. (b) Andersson, M. P.; Uvdal, P. L. *J. Phys. Chem. A* **2005**, *109*, 3937.

(34) Bencheikh, M.; Koivisto, R.; Launila, O.; Flament, J. P. *J. Chem. Phys.* **1997**, *106*, 6231.

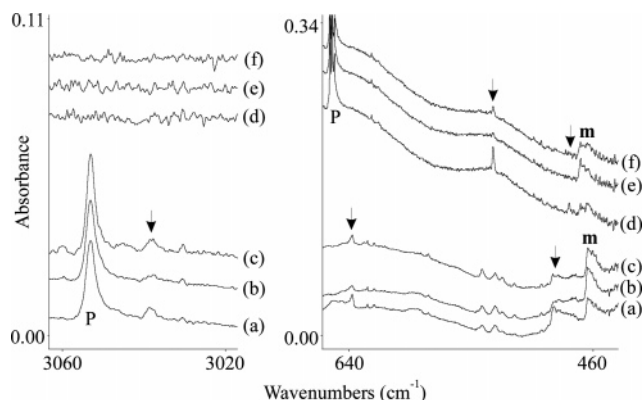(35) Blinova, O. V.; Shklyarik, V. G.; Shcherbe, L. D. *Zh. Fz. Khim.* **1988**, *62*, 1640.

Figure 2. Infrared spectra in selected regions for laser-ablated Cr atom and CHCl$_3$ reaction products with 0.5% reagent in argon co-deposited for 1 h at 8 K. (a) CHCl$_3$. (b) After irradiation (λ < 220 nm). (c) After annealing to 30 K. (d) CDCl$_3$. (e) After irradiation (λ > 220 nm). (f) After annealing to 30 K. Arrows denote the methylidyne absorptions, and P denotes precursor bands.

New absorptions and calculated frequencies using both B3LYP and BPW91 density functionals are compared in Table S3 for the triplet ground-state CH$_2$=CrFCl molecule, and the agreement confirms this identification. In addition, evidence is found for the quintet CH$_2$Cl–CrF insertion product at 545.8 and 642.8 cm^{-1}, which is calculated to be 6 kcal/mol more stable than the CH$_2$F–CrCl analogue. These observed frequencies correspond to calculated CH$_2$ rocking (558 cm^{-1}, 16 km/mol intensity) and Cr–F stretching (648 cm^{-1}, 181 km/mol) modes, and the latter shifts to 635.9 cm^{-1} for CD$_2$Cl–CrF (642 cm^{-1}, 178 km/mol). Satisfactory matching of the observed and calculated Cr–F stretching mode position and small deuterium shift confirms the identification of the CH$_2$Cl–CrF insertion product and the mechanism for the more energetically favorable insertion at the C–F rather than the C–Cl bond. Finally, the CH$_2$Cl–CrF insertion product has a Cl bridged structure similar to that of CH$_2$Cl–CrCl.

$$Cr^* + CH_2FCl \rightarrow CH_2Cl–CrF^* \rightarrow CH_2=CrFCl \quad (1c)$$
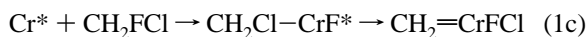
Cr + CHX$_3$. The chloroform reaction revealed two sets of product bands. The first bands at 3038.5, 637.8, and 488.9 cm^{-1} decreased by 50% on >290 nm and another 20% on >220 nm irradiations and then increased 2-fold on annealing to 30 K, and decreased in concert by 50% on the final full arc irradiation as shown in Figure 2. Another band at 463.6 cm^{-1} increased on UV irradiation, while the first set decreased. The two lower bands contain unresolved red shoulders for chlorine isotopic components of a species with two or more chlorine atoms. The chloroform-*d* absorptions for the first photosensitive set were observed at 533.7 and 477.6 cm^{-1}, and the second band increased at 469.3 cm^{-1}. The highest frequency component is lost under the strong precursor C–D stretching band based on the expected deuterium shift.

Our B3LYP calculations find the triplet methylidene CHCl=CrCl$_2$ to have its strongest infrared absorption at 475.1 cm^{-1} with a deuterium counterpart blue-shifted to 479.8 cm^{-1} due to interaction with a weaker hydrogen deformation mode, which are in good agreement with our 463.6 and 469.3 cm^{-1} bands. A quintet state with a 90° dihedral angle is 1 kcal/mol lower in energy, but the antisymmetric Cr–Cl mode is too low at 457 cm^{-1} and red shifts 10 cm^{-1} with deuterium. Furthermore, higher spin states are favored by the B3LYP calculation.[36] An

analogous calculation locates a trigonal HC≡CrCl$_3$ molecule 14 kcal/mol higher in energy with the frequencies listed in Table 2. The 3038.5 cm^{-1} band is the lowest C–H stretching mode we have observed for a methylidyne complex. The calculation predicts this mode 4.8% too high, which is almost the same as the 4.7% too high computation for the C–H frequency of CH$_2$=CrCl$_2$, and both are appropriate for the B3LYP functional.[33] The degenerate H–C–Cr deformation mode calculated at 662.8 cm^{-1} is observed as a sharp band at 637.8 cm^{-1} with D–C–Cr counterpart at 533.7 cm^{-1} (ratio 1.195). The degenerate Cr–Cl stretching mode computed at 475.2 cm^{-1} is observed slightly higher at 488.9 cm^{-1} with deuterium counterpart at 477.6 cm^{-1}. Unfortunately, the C≡Cr stretching mode is calculated with zero infrared intensity, and we observed no absorption in the 1000–1050 cm^{-1} region for this band. The correlation between calculated and observed frequencies for the HC≡CrCl$_3$ methylidyne molecule (Table 2) substantiates its present formation and characterization. With highly exothermic reactions like those under investigation here, it is common to produce and trap molecules that are slightly higher than the global minimum energy product.[19–21]

This reaction also begins with insertion and then is followed by α-chlorine transfer to chromium to form the methylidene and the methylidyne complexes. The reaction to give the methylidene releases 67 kcal/mol, and the overall reaction 2 to form the methylidyne complex is 53 kcal/mol exothermic. These reactions are likely initiated by chromium atoms excited in the laser-ablation process and sustained by the reaction exothermicities.

$$Cr^* + CHCl_3 \rightarrow CHCl_2–CrCl^* \rightarrow CHCl=CrCl_2^* \rightarrow$$
$$HC≡CrCl_3 \quad (2)$$
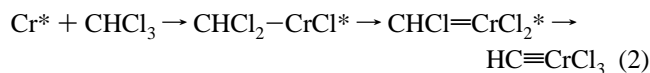
The fluoroform reaction also gave two products, first with bands at 758.7, 670.3, and 630.5 cm^{-1} and the second with stronger absorptions at 753.8, 655.5, and 649.7 cm^{-1} bands, which shifted using fluoroform-*d* to 758.2, 667.8, and 531.8 cm^{-1} and to 753.2, 652.9, and 541.9 cm^{-1}. Infrared spectra in Figure S3 show that the first bands increased 60% and the second set 300% on >290 and >220 nm irradiations. The first group of absorptions and deuterium counterparts corresponds with the three strongest bands calculated for the triplet CHF=CrF$_2$ methylidene product, which is 44 kcal/mol lower in energy than the reagents. These frequencies computed at 762.6, 668.8, and 627.5 cm^{-1} are antisymmetric and symmetric Cr–F stretching and C–H wagging modes, which shift to 762.3, 667.3, and 528.0 cm^{-1} on deuteration (the strong C–F mode predicted at 1168 cm^{-1} is covered by precursor).

The two strongest absorptions in the second group at 753.8 and 655.5 cm^{-1} are antisymmetric and symmetric Cr–F stretching modes, which are predicted by our calculation for trigonal HC≡CrF$_3$ at 770.7 and 684.9 cm^{-1}, and for DC≡CrF$_3$ at 769.7 and 683.5 cm^{-1} (Table 2). The degenerate H–C–Cr bending mode calculated at 622.3 cm^{-1} is observed at 649.7 cm^{-1} with D–C–Cr counterpart at 541.9 cm^{-1} (ratio 1.199). The B3LYP calculation is 2.2% and 4.5% high for the Cr–F stretching modes, as is typical for this functional,[33] but is 4.2% low for the more difficult to model bending mode. The exothermic reaction to form CHF=CrF$_2$ promotes another α-fluorine transfer to the 13 kcal/mol higher energy HC≡CrF$_3$ product in these laser ablation experiments.

Cr + CX$_4$. Infrared spectra following the Cr and CCl$_4$ reaction revealed absorptions at 1230.6 cm^{-1}, with a weaker 1228.2 cm^{-1} shoulder, and at 495.7 cm^{-1} that decreased 60% together on >290 nm irradiation and another 10% on >220

(36) Swart, M. *Inorg. Chim. Acta* **2007**, *360*, 179.

Table 2. Observed and Calculated Fundamental Frequencies of HC≡CrX₃ Complexes in the Ground $^1A_1$ Electronic State with C_{3v} Structure^a

approximate description	HC≡CrCl₃			DC≡CrCl₃			HC≡CrF₃			DC≡CrF₃		
	obs	calc	int	obs	calc	int	obs	calc	int	obs	calc	int
C−H str, a₁	3038.5	3183.9	31	covered	2365.1	31	covered	3190.8	39	covered	2369.3	22
HC≡Cr str, a₁		1054.9	0		1013.5	0		1047.8	7		1008.5	7
Cr−X str, e	488.9	475.2	79 × 2	477.6	468.7	62 × 2	753.8	770.7	200 × 2	753.2	769.7	187 × 2
Cr−X str, a₁		390.1	7		389.5	7	655.5	684.9	59	652.9	683.5	58
H−C−Cr def, e	637.8	662.8	68 × 2	533.7	533.7	58 × 2	649.7	622.3	29 × 2	541.9	532.1	12 × 2
C−Cr−X def, e		234.4	15 × 2		212.3	7 × 2		294.2	16 × 2		251.4	14 × 2
Cr−X₃ umb, a₁		168.6	0		143.7	0		274.0	8		273.3	8
Cr−X₂ bend, e		118.4	0		100.4	0		197.5	4 × 2		197.5	4 × 2

^{a} Frequencies and intensities are in cm^{-1} and km/mol. Observed in an argon matrix. Frequencies and intensities computed with B3LYP/6-311++G(2d,p) in the harmonic approximation using the SDD core potential and basis set for Cr. Symmetry notations are based on the C_{3v} structure.
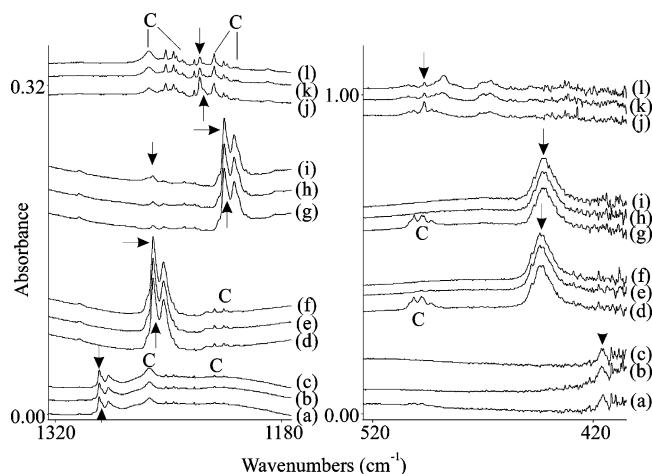

Figure 3. Infrared spectra in selected regions for the group 6 metal atom and CCl₄ reaction products in excess argon at 8 K. 0.5% reagent co-deposited for 1 h with (a) W, (d) Mo, (g) Mo and ^{13}-CCl₄ (90% enriched), and (j) Cr spectra (b), (e), (h), and (k) after irradiation ($\lambda > 290$ nm). Spectra (c), (f), (i), and (l) after irradiation ($\lambda > 220$ nm). C denotes bands common to experiments with different metals. Arrows denote the methylidyne complex absorptions.

nm irradiation. Additional absorptions for different species appeared at 859.3, 487.7, and 466.6 cm^{-1} on irradiation. This spectrum is compared to spectra from Mo and W reactions in Figure 3. Carbon-13 substitution shifted the former bands to 1189.3 and 495.9 cm^{-1}.

The strongest absorptions predicted by B3LYP calculations for the ClC≡CrCl₃ complex are the antisymmetric Cl−C−Cr stretching and Cr−Cl stretching modes at 1258.5 and 484.6 cm^{-1}, respectively, which correlate very well with our photosensitive product absorptions at 1230.6 and 496.5 cm^{-1}. The 41.3 cm^{-1} carbon-13 shift is more than that for a harmonic diatomic oscillator, but the 2.4 cm^{-1} shift to the weaker shoulder appropriate for chlorine-37 in natural abundance is less than that for the diatomic model. Hence, these complementary shifts characterize the antisymmetric Cl−C−Cr stretching vibration, which depends more on the carbon reduced mass. Furthermore, the relative intensities of the chlorine isotopic peaks and the residual carbon-12 in the 90% carbon-13-enriched sample characterize the vibration of single C and Cl atoms. The 496.5 cm^{-1} band has red shoulders appropriate for the vibration of two or more chlorine atoms. The above absorptions make a strong case for identification of the ClC≡CrCl₃ molecule.

The 859.3 and 466.6 cm^{-1} absorptions that increase on the >290 nm irradiation when ClC≡CrCl₃ absorptions decrease are appropriate for the strongest C−Cl stretching mode and Cr−Cl stretching mode of the quintet ground-state methylidene

CCl₂−CrCl₂ complex, which is 6 kcal/mol lower in energy than the triplet methylidene CCl₂=CrCl₂ complex and 11 kcal/mol lower than the ClC≡CrCl₃ product. These modes are calculated at 884 and 456 cm^{-1}, which correlate with the observed bands.

The reaction with CF₄ produced weak bands at 1475.9, 765.7, and 759.1 cm^{-1}, which increased slightly on >290 nm irradiation and were affected little by >220 nm irradiation. The bands near 760 cm^{-1} are appropriate for Cr−F vibrations, but the 1475.9 cm^{-1} band is lower than our prediction (Table S4) for the antisymmetric F−C−Cr stretching mode for the FC≡CrF₃ complex [this band is probably covered by the intense precursor absorption at 1550−1530 cm^{-1}].

Investigations were done with Freon compounds because they are more reactive than CF₄, and we have already synthesized the carbon-13 precursors.[31] Figure S4 compares spectra from the Mo and Cr reactions with CF₂Cl₂, which give very different product yields, and spectra from Cr with CF₃Cl. Notice first the strong 1521.6 [1475.7] cm^{-1} band with Mo that increases markedly on both UV irradiations, and then find the weak 1528.3 [1483.5] and 1481.8 [1438.5] cm^{-1} bands with Cr [the lower band is marked with the lighter arrow], which show opposite behavior on the two UV irradiations, and the very strong 1303.1 and 1261.3 cm^{-1} bands [carbon-13 counterparts given in square brackets], which exhibit a still different behavior on irradiation. The lower region reveals weaker 443.4 [441.1] and 697.8 [693.8] cm^{-1} bands, which track with the very strong bands all increasing 35% on >290 nm and none on >220 nm irradiations. In addition, weaker new bands appear at 830.9 [805.3] and 488.5 [488.5] cm^{-1} on >220 nm irradiation.

It is clear from the carbon-13 shift percentages, 2.93% and 2.92%, that the weak CF₂Cl₂ product bands at 1528.3 and 1481.8 cm^{-1} are due to antisymmetric F−C−Cr vibrations for a linear linkage. The FC≡CrFCl₂ complex is predicted to have a very strong antisymmetric F−C−Cr stretching vibration at 1565.7 cm^{-1} (Table S4) with a 2.96% carbon-13 shift, and such agreement is sufficient to identify this methlyidyne complex. The stronger 1481.8 cm^{-1} band is best identified as a photoreversible structural isomer of this same species. The matrix cage may assist in the stabilization of these two isomers. Although the other positional isomer, ClC≡CrF₂Cl, is 2 kcal/mol more stable, the strong Cl−C−Cr mode is predicted at 1259 cm^{-1} in a region covered with precursor absorptions, which preclude its detection.

The very strong 1303.1 and 1261.3 cm^{-1} bands also show carbon-13 shifts, 2.56% and 2.57%, that are appropriate for antisymmetric C−F stretching modes, but with less carbon participation that comes with a smaller valence angle. The CF₂-CrCl₂ methylidene products were computed, and the quintet was found to be 13 kcal/mol lower in energy than the triplet state and to have very strong antisymmetric and symmetric C−F
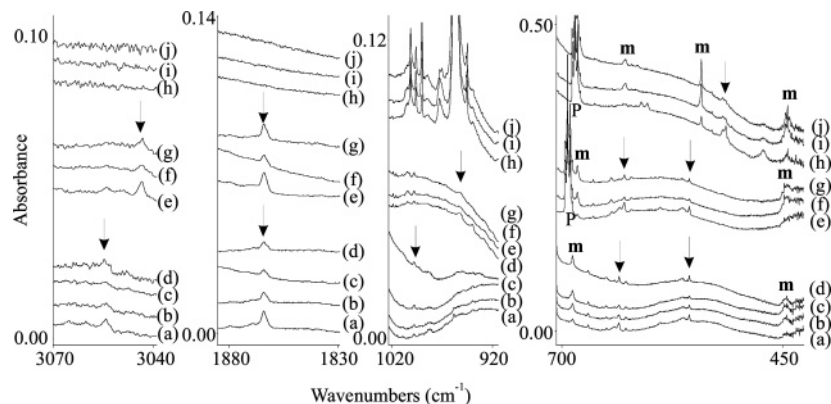
Figure 4. Infrared spectra in selected regions for the Mo atom and CH_2Cl_2 reaction products in excess argon at 8 K. (a) Mo + 0.5% CH_2Cl_2 in argon co-deposited for 1 h. (b) After irradiation (λ < 290 nm). (c) After irradiation (λ > 220 nm). (d) After annealing to 30 K. (e) Mo + 0.5% $^{13}CH_2Cl_2$ in argon co-deposited for 1 h. (f) After irradiation (λ > 220 nm). (g) After annealing to 30 K. (h) Mo + 0.5% CD_2Cl_2 in argon. (i) After irradiation (λ > 220 nm). (j) After annealing to 30 K [bands in 900 cm^{-1} region are common with this precursor with all metals]. The lable **m** denotes methylidene, arrows indicate the methylidyne complex absorption, and P denotes precursor bands.

Table 3. Observed and Calculated Fundamental Frequencies of CH_2=$MoCl_2$ in the Ground $^3A_2$ Electronic State with C_{2v} Symmetry[a]

approximate description	CH_2=$MoCl_2$			$^{13}CH_2$=$MoCl_2$			CD_2=$MoCl_2$		
	obs	calc	int	obs	calc	int	obs	calc	int
C−H str, b_2		3170.3	1		3157.8	1		2354.9	1
C−H str, a_1		3066.3	17		3061.0	16		2221.0	15
HCH bend, a_1		1298.0	8		1288.0	7		1027.5	18
CH_2 wag, b_1	688.1	735.3	88	682.4	729.0	86	542.2	575.5	54
C=Mo str, a_1	−[b]	729.0	35	−[b]	710.3	35	628.3	642.3	23
Mo−Cl str, b_2	446.0	454.1	98	444.9	452.6	99	444.6	444.2	103
CH_2 twist, a_2		438.8	0		438.8	0		311.4	0
Mo−Cl str, a_1		376.2	25		376.0	25		375.7	25

[a] Frequencies and intensities are in cm^{-1} and km/mol. Four lower real frequencies are not listed. Observed in an argon matrix. Symmetry notations are based on the C_{2v} structure. Frequencies and intensities computed with B3LYP/6-311++G(2d,p) in harmonic approximation using the SDD core potential and basis set for Mo. [b] Band covered by precursor.

stretching modes at 1276.6 and 1238.6 cm^{-1} with 2.62% carbon-13 shifts, a weaker 690.6 cm^{-1} band with 4.1 cm^{-1} carbon-13 displacement, and a strong Cr−Cl stretching mode at 441.0 cm^{-1} with 3.5 cm^{-1} carbon-13 shift (Table S5). Considering the approximations involved, although the B3LYP functional favors higher spin states,[30] the 1303.1, 1261.3, 697.8, and 443.3 cm^{-1} bands and carbon-13 shifts correlate very well and identify this major product as the quintet CF_2−$CrCl_2$ methylidene. In contrast, the higher energy triplet methylidene calculated frequencies do not fit our observations [the Cr−Cl stretch is too high at 492 cm^{-1} and the symmetric C−F stretch is too low at 1156 cm^{-1}]. The weaker 830.9 and 488.5 cm^{-1} bands are most likely due to C−F and Cr−Cl stretching modes in the isomer quintet CFCl−CrFCl complex, which is calculated to be 9 kcal/mol higher in energy. Based on our experience with halomethane reactions, the methylidene reaction product is expected to be a major product in these systems. What is important here is that the major lower oxidation state quintet methylidene product is 24 kcal/mol lower in energy then the minor singlet FC≡CrFCl$_2$ methylidyne product. The absorptions observed with CF$_3$Cl support these identifications.

The reaction of Cr with CX$_4$ molecules proceeds as given for the favorable CCl$_4$ example, where the overall reaction is exothermic by 73 kcal/mol. The reaction

$$Cr^* + CCl_4 \rightarrow CCl_3-CrCl^* \rightarrow CCl_2-CrCl_2^* \rightarrow$$
$$ClC\equiv CrCl_3 \quad (3)$$
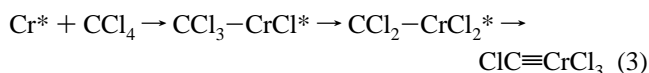
passes through the quintet insertion product with α-chlorine transfer to form the quintet methylidene and a second α-chlorine transfer to give the final methylidyne product. The corresponding

CF$_4$ reaction is exothermic by only 31 kcal/mol, and the product yield is much lower than that for CCl$_4$. The chlorofluorocarbon reactions appear to go through C−Cl insertion followed by successive α-halogen transfers.

Mo + CH$_2$X$_2$. The reactions of laser-ablated molybdenum atoms and methylene chloride are shown in Figure 4 for four diagnostic regions. The sharp bands marked with arrows at 3054.6, 1864.4, 635.4, and 555.8 cm^{-1} and a broad band centered at 983 cm^{-1} decrease 50% on >290 nm irradiation, decrease 10% more on >220 nm irradiation, and increase 30% on annealing to 30 K to allow diffusion. On the other hand, new bands labeled **m** at 688.1, 446.0, and 443.1 cm^{-1} increase 50% on >290 nm irradiation, another 20% on >220 nm irradiation, and do not change on the final 30 K annealing. These new absorptions shift with $^{13}CH_2Cl_2$ and CD_2Cl_2 as given in Tables 3 and 4. A new **m** band is observed at 628.3 cm^{-1} with CD_2Cl_2, which suggests that the CH_2Cl_2 counterpart is covered by strong precursor absorption near 750 cm^{-1}.

The analogous reaction with methylene fluoride gave similar spectra with new absorptions at 665.8 and 639.1 cm^{-1} that showed little change on irradiation and new bands that appeared on >290 nm irradiation at 1883.4, 973.3, 704.7, 658.8, 610.6, and 561.3 cm^{-1}. With CD_2F_2, two bands at 664.6 and 643.5 cm^{-1} were unchanged on irradiation, and the first three bands produced on photolysis shifted to 1355.1, 932.0, and 692.8 cm^{-1}, as listed in Tables S6 and S7.
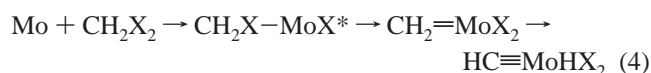
Extensive experience with transition metal atom and halomethane reactions suggests that C−X insertion followed by

Table 4. Observed and Calculated Fundamental Frequencies of the HC≡MoHCl₂ Complex in the Ground ¹A′ Electronic State with C_s Structure[a]

approximate description	HC≡MoHCl₂			H¹³C≡MoHCl₂			DC≡MoHCl₂		
	obs	calc	int	obs	calc	int	obs	calc	int
C−H str, a′	3054.6	3205.8	24	3043.4	3194.0	24	2293.2	2383.2	19
Mo−H str, a′	1864.4	1980.4	96	1864.2	1980.4	96	1340.7	1409.0	51
C≡Mo str, a′	983	1051.7	11	952	1019.0	75	938	1005.2	9
Mo−H def, a′		811.6	5		804.4	65		640.9	5
H−C−Mo def, a′	635.4	629.3	90	629.4	623.0	69	514.6	507.5	77
H−C−Mo def, a″	555.8	581.0	55	555.6	580.5	16		465.8	50
Mo−H def, a″		578.8	26		578.8	47		419.5	18
Mo−Cl, str, a″		409.8	69		409.7	70		379.5	32
Mo−Cl str, a′		384.1	24		384.0	24		360.3	19

[a] Frequencies and intensities are in cm⁻¹ and km/mol. Three lower real frequencies are not listed. Observed in an argon matrix. Frequencies and intensities computed with B3LYP/6-311++G(2d,p) in the harmonic approximation using the SDD core potential and basis set are for Mo. The symmetry notations are based on the C_s structure.

α-halogen transfer reactions occur to saturate the metal center as summarized in reaction 1.[10−13,16−21]

$$\text{Mo} + \text{CH}_2\text{X}_2 \rightarrow \text{CH}_2\text{X}-\text{MoX}^* \rightarrow \text{CH}_2=\text{MoX}_2 \rightarrow$$
$$\text{HC}\equiv\text{MoHX}_2 \quad (4)$$

For the first example of Mo and CH₂Cl₂, the quintet state insertion product is 73 kcal/mol lower in energy than the reagents, but the triplet methylidene is 29 kcal/mol lower in energy than the insertion product, and the singlet methylidyne is an additional 5 kcal/mol higher in energy so all of these are accessible based on the exothermicity of the insertion step (73 kcal/mol) as represented by the asterisk. The quintet CH₂−MoCl₂ is 21 kcal/mol higher than the triplet methylidene, so this is an unlikely contributor to the product spectrum. In addition, the strongest calculated mode, the antisymmetric Mo−Cl stretch, is 31 cm⁻¹ below the observed band, and such is not appropriate. Finally, the reaction to form the triplet methylidene is 102 kcal/mol exothermic, and the overall reaction 1 to form the singlet methylidyne is exothermic by 98 kcal/mol.

The spectra in Figure 4 show two products, which exhibit opposite behavior on UV irradiation. The **m** bands that increase include a 446.0 cm⁻¹ band with a 443.1 cm⁻¹ component of one-half the intensity, which is appropriate for natural chlorine isotopic splitting. The calculated complete chlorine 35−37 shift for the antisymmetric vibration of a MoCl₂ subunit with the 125.8° angle calculated here for triplet CH₂=MoCl₂ is 6.4 cm⁻¹, and the isotopic splitting for the Mo³⁵Cl₂ and Mo³⁵Cl³⁷Cl species in a 9/6 population ratio is expected near one-half of the complete shift or 3.2 cm⁻¹, which is in very good agreement with the 2.9 cm⁻¹ observed splitting. Hence, the 446.0 cm⁻¹ band is due to the antisymmetric vibration of an MoCl₂ subunit. The 688.1 cm⁻¹ band shifts 5.7 cm⁻¹ with carbon-13 and to 542.2 cm⁻¹ on deuteration, which are appropriate for the CH₂ wagging mode that appears at 659.4 cm⁻¹ in the CH₂=MoHCl complex.[20] Furthermore, a new band appears at 628.3 cm⁻¹ for the deuteriated species, which must arise from a product with a hydrogen counterpart masked by the strong precursor absorption in the low 700 cm⁻¹ region. Our B3LYP calculation (Table 3) for the CH₂=MoCl₂ complex places this C=Mo stretching mode appropriately. Hence, the three vibrations characterized here by isotopic shifts identify MoCl₂, CH₂, and C=Mo subunits that define the CH₂=MoCl₂ complex, and the excellent correlation between the observed and strongest calculated infrared frequencies confirms these assignments.

The bands marked by arrows decrease on irradiation, but increase on subsequent annealing of the argon matrix sample, which suggests a spontaneous reaction to form a stable product.

This five-band set also includes diagnostic modes that identify the product. The sharp band at 3054.6 cm⁻¹ shifts to 3043.3 cm⁻¹ with carbon-13 and to 2293.2 cm⁻¹ with deuterium, which describes a C−H vibration (H/D frequency ratio 1.3320). The sharp 1864.4 cm⁻¹ absorption shifts negligibly with carbon-13 and significantly to 1340.7 cm⁻¹ with deuterium (H/D ratio 1.3906), which characterizes a Mo−H vibration. Similar modes have been observed at 1840.7 and 1835.8 cm⁻¹ for the HC≡MoH₂Cl complex.[20] The 983 cm⁻¹ band has the profile for natural molybdenum isotopes, which will be discussed in detail for the resolved HC≡MoCl₃ case below. This band shifts 31 cm⁻¹ with carbon-13 and 45 cm⁻¹ with deuterium, which are in good agreement with our calculated frequencies for a HC≡Mo stretching mode (Table 4). The sharp 635.4 cm⁻¹ band shifts 6.0 cm⁻¹ with carbon-13 and to 514.6 cm⁻¹ (H/D ratio 1.2348) with deuterium, which is appropriate for a H−C−Mo deformation mode. Finally, the sharp 555.8 cm⁻¹ band shows a very small carbon-13 shift, and the deuterium counterpart is below our instrumental cutoff, as it falls just below 572.8, 568.2 cm⁻¹ bands for Mo−H deformation modes in the HC≡MoH₂-Cl complex. In summary, the excellent correlation between observed absorptions and calculated isotopic frequencies and intensities (Table 4) confirms the present identification of the methylidyne molecule HC≡MoHCl₂.

Methylene fluoride produced weaker bands with photochemistry different from that of methylene chloride. The bands at 665.8 and 639.1 cm⁻¹ are the strongest and third strongest of the bands calculated for CH₂=MoF₂, and the strongest for CD₂=MoF₂ shifts only slightly to 664.6 cm⁻¹ as these are antisymmetric MoF stretching modes. The CD₂ wagging mode is observed at 643.5 cm⁻¹, but the CH₂ counterpart is covered by strong precursor absorptions. Following the above identification of CH₂=MoCl₂, these bands are sufficient to show that CH₂=MoF₂ is formed in the Mo reaction with CH₂F₂.

The second set of absorptions produced on near-UV irradiation includes bands that identify this new product as HC≡MoHF₂, which is calculated to be 4 kcal/mol higher in energy than the triplet methylidene. Unfortunately, the C−H stretching mode falls under precursor in this case, but the Mo−H stretching mode is observed at 1883.4 cm⁻¹ with D counterpart at 1355.1 cm⁻¹ (H/D ratio 1.3899). The strongest band, the antisymmetric Mo−F stretching mode at 704.7 cm⁻¹, shifts to 692.8 cm⁻¹ with deuterium. The weaker symmetric Mo−F stretching mode and antisymmetric H−C−Mo and symmetric Mo−H deformation modes are also observed (Table S7) for the hydrogen compound. Again, the correlation between observed and calculated spectra confirms the assignments.

Mo + CHX₃. Infrared spectra from the series of HCFₙCl₃₋ₙ (n = 0, 1, 2, 3) haloform reactions with laser-ablated molyb-
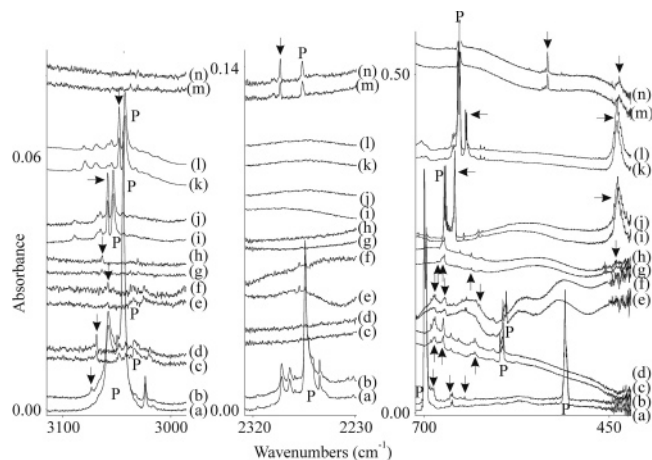
Figure 5. Infrared spectra in selected regions for laser-ablated Mo atom and CHX_3 reaction products with 0.5% reagent in argon co-deposited for 1 h at 8 K and after full arc irradiation. (a) CHF_3. (b) After irradiation (λ < 220 nm). (c) CHF_2Cl. (d) After irradiation. (e) $^{13}CHF_2Cl$. (f) After irradiation. (g) $CHFCl_2$. (h) After irradiation. (i) $CHCl_3$. (j) After irradiation. (k) $^{13}CHCl_3$. (l) After irradiation. (m) $CDCl_3$. (n) After irradiation. Arrows denote the methylidyne absorptions, and P denotes precursor bands.
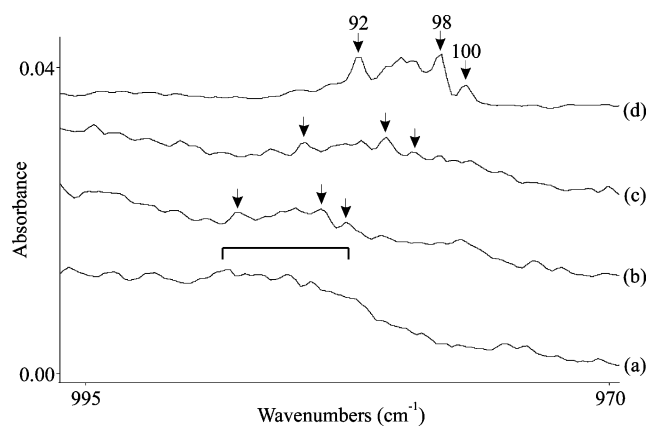

Figure 6. Infrared spectra in the 995−970 cm^{-1} region for the laser-ablated Mo atom and CHX_3 reaction products with 0.5% reagent in argon co-deposited for 1 h at 8 K and subjected to ultraviolet irradiation. (a) CHF_3, (b) CHF_2Cl, (c) $CHFCl_2$, and (d) $CHCl_3$. Arrows indicate resolved Mo 92, 98, and 100 isotopic bands.

denum atoms are illustrated in Figure 5 where the first set of spectra shows new C−H stretching modes marked by arrows. Also included are spectra from the reactions of $^{13}CHF_2Cl$, ^{13}-$CHCl_3$, and $CDCl_3$ where the isotopic shifts characterize C−H vibrations. The lower region displays the common H−C−Mo deformation mode and Mo−F and Mo−Cl stretching vibrations, and the observed frequencies are listed in Tables 5 and S8. The weak fluoroform reaction product doubled on full arc irradiation, did not change on annealing to 30 K, and doubled again on a second full arc irradiation. The strong chloroform product increased 10% on the first full arc irradiation, 20% on annealing, and another 10% on the second irradiation.

Figure 6 shows spectra in the 980 cm^{-1} region where natural molybdenum[37] isotopic splittings are resolved in the high yield chloroform product (982.0, 980.7, 980.0, 979.4, 978.1, and 976.9 cm^{-1} for Mo 92, 94, 95, 96, 98, and 100, respectively) and partially resolved for the $CHFCl_2$ product at 984.6, 980.7, and 979.4 cm^{-1} marked by arrows for the major isotopes Mo 92,

98, and 100, respectively, and for the CHF_2Cl product at 987.8, 983.8, and 982.6 cm^{-1}. [The Mo 92 to 100 separations are 5.1, 5.2, and 5.2 cm^{-1} in these three sets of data.] A broad band centered at 986 cm^{-1} is observed for the CHF_3 product. Notice the trend of increased C≡Mo stretching frequency with increased fluorine substitution, which is predicted by our calculations (Tables 5 and S8). Molybdenum isotopic resolution was equally as good with $^{13}CHCl_3$ where Mo isotopic peaks were observed at 952.1, 950.7, 950.0, 949.3, 948.0, and 946.8 cm^{-1}, respectively. Notice that the latter Mo 92 to 100 isotopic separation of 5.3 cm^{-1} is larger than the value for the carbon-12 product as Mo vibrates more against the heavier carbon isotope.

The resolved molybdenum isotopic splittings convincingly demonstrate that a single Mo atom participates in this vibrational mode. The Mo 92 to 100 separation for the chloroform product, 5.1 cm^{-1}, is less than the 6.3 cm^{-1} adjusted value found for MoN and the 6.0 cm^{-1} average value for the two stretching modes of $(O_2)MoO_2$ as these mass partners are heavier, and the latter gives strong, completely resolved Mo isotopic spectra.[38,39] For a harmonic diatomic C−Mo oscillator, the Mo 92 to 100 isotopic shift at 978.1 cm^{-1} would be 4.6 cm^{-1}, which is slightly less than our 5.1 cm^{-1} observed value, and this shift for C 13 against Mo 98 would be 34.2 cm^{-1}, which is slightly more that our 30.1 cm^{-1} observed value. This means that the Mo atom is also coupled slightly to the three Cl atoms and that Mo moves in an antisymmetric fashion between HC and three Cl atoms in this mode. For the major Mo-98 isotope, a simple C−Mo diatomic oscillator would shift from 978.1 to 943.9 cm^{-1} on carbon-13 substitution, a shift some 1.4 cm^{-1} more than that calculated for the anticipated HC≡$MoCl_3$ product (Table 5). This difference arises because the C−H mode interacts slightly and DC produces an even larger 45.7 cm^{-1} observed and 46.1 cm^{-1} calculated shift for the DC≡$MoCl_3$ product absorption. So our B3LYP calculations predict the Mo isotopic shift within 0.1 cm^{-1} and demonstrate that we are dealing with the HC≡Mo stretching mode of a carbyne species. The triple bond stretching mode of acetylene itself exhibits an even larger deuterium isotopic shift.[40]

The stronger band at 3058.2 cm^{-1} shifts to 3048.0 cm^{-1} on carbon-13 and to 2296.2 cm^{-1} on deuterium substitution (H/D ratio 1.3319), which are appropriate for a C−H stretching mode. The very strong, very sharp 658.9 cm^{-1} band shifts to 652.4 cm^{-1} with carbon-13 and to 533.4 cm^{-1} with D (H/D ratio 1.2353), which characterizes the degenerate H−C−Mo deformation mode, and the absence of splitting on this band verifies that the C_{3v} symmetry of the molecule is maintained in the matrix. The strong 438.7 cm^{-1} band is appropriate for the degenerate Mo−Cl stretching mode. Density functional calculations using B3LYP typically overshoot vibrational frequencies, and the C−H mode is calculated 5.0% too high by the B3LYP functional, as is expected,[33] but for more difficult to model modes, the HC≡Mo mode is calculated 7.6% too high, the deformation mode 0.12% high, and the Mo−Cl stretching mode 3.0% too low. The calculation of vibrational frequencies, particularly for a Mo carbyne, is not an exact science, and we expect density functional theory to provide a very good

(37) *CRC Handbook*; Chemical Rubber Publishing Co.: Boca Raton, FL, 1985.

(38) Andrews, L.; Souter, P. F.; Bare, W. D.; Liang, B. *J. Phys. Chem. A* **1999**, *103*, 4649 (MoN).

(39) Bare, W. D.; Souter, P. F.; Andrews, L. *J. Phys. Chem. A* **1998**, *102*, 8279 (MoO₂).

(40) Herzberg, G. *Infrared and Raman Spectra*; D. Van Nostrand; Princeton, NJ, 1945.

Table 5. Observed and Calculated Fundamental Frequencies of HC≡MoX₃ Complexes in the Ground $^1A_1$ Electronic State with C_{3v} Structure[a]

approximate description	HC≡MoCl₃			H¹³C≡MoCl₃		DC≡MoCl₃			HC≡MoF₃		
	obs	calc	int	obs	calc	obs	calc	int	obs	calc	int
C−H str, a₁	3058.2	3212.2	35	3048.0	3200.4	2296.2	2387.9	24	3073.1	3221.2	39
HC≡Mo str, a₁	978.1[b]	1051.9	8	948.0	1019.1	932.4[b]	1005.8	6	986.0[c]	1065.0	20
Mo−X str, e	438.7	425.0	81 × 2	438.6	425.4	436.4	423.0	74 × 2	689.2	683.4	210 × 2
Mo−X str, a₁		380.8	9		380.7		380.7	9	664.6	651.7	60
H−C−Mo def, e	658.9	660.2	76 × 2	652.4	653.4	533.4	533.6	52 × 2	645.4	642.7	30 × 2
C−Mo−X def, e		237.7	7 × 2		232.5		212.3	7 × 2		288.7	5 × 2
Mo−X₃ umb, a₁		144.0	0		143.7		143.7	0		228.0	9
Mo−X₂ bend, e		100.4	0		100.4		100.4	0		163.6	8 × 2

[a] Frequencies and intensities are in cm⁻¹ and km/mol. Observed in an argon matrix. Frequencies and intensities computed with B3LYP/6-311++G(2d,p) in the harmonic approximation using the SDD core potential and basis set for Mo. The symmetry notations are based on the C_{3v} structure. [b] Band position for the major ⁹⁸Mo isotope: see Figure 3. [c] Band center: see Figure 3.

Table 6. Observed and Calculated Fundamental Frequencies of XC≡MoX₃ Complexes in the Ground $^1A_1$ Electronic State with C_{3v} Structure[a]

approximate description	ClC≡MoCl₃			Cl¹³C≡MoCl₃			FC≡MoF₃		
	obs	calc	int	obs	calc	int	obs	calc	int
anti X−C≡Mo str, a₁	1259.6	1278.6	165	1215.6	1233.1	154	1524.2	1566.3	353
sym X−C≡Mo str, a₁		453.7	25		453.6	25		619.0	1
anti Mo−X str, e	443.6	432.0	96 × 2	430.2	653.5.0	98 × 2	682.3	677.8	169 × 2
X−C−Mo def, e		382.5	3 × 2		370.5	1 × 2		464.8	2 × 2
sym Mo−X str, a₁		371.8	8		372.0	7	664.3	658.8	103
Mo−X₃ umb, a₁		130.7	0		130.5	0		218.3	8
C−Mo−X def, e		99.1	0		99.0	0		161.9	8 × 2
Mo−X₂ bend, e		78.5	0		78.5	0		142.9	0

[a] Frequencies and intensities are in cm⁻¹ and km/mol. Observed in an argon matrix. Frequencies and intensities computed with B3LYP/6-311++G(2d) in the harmonic approximation using the SDD core potential and basis set for Mo. The symmetry notations are based on the C_{3v} structure.

approximation for frequencies and a good approximation for infrared intensities, and this is in fact achieved here for HC≡MoCl₃.

Five absorptions in the CHF₃ reaction correlate well with the above CHCl₃ product bands, and the calculated frequencies (Table 5) support the assignment to HC≡MoF₃. The Mo−F stretching modes are, of course, higher than the Mo−Cl counterparts, and the C−H stretching and H−C−Mo deformation modes show slight changes. The trend in C−H stretching mode will be later related to hybridization of carbon in these molecules.

The ability to tune the C−H stretching frequency with halogen substituents at the metal center prompted inclusion of the fluorochloroform precursors with this investigation. The Mo−F and Mo−Cl stretching modes of the latter reaction products are near the values discussed above (Tables 5 and S8). The H−C−Mo deformation modes do not form a smooth trend because the now nondegenerate stretching and deformation modes mix more in the molecules with lower symmetry although the average of the two deformation modes for the F, Cl species falls between the values for the trigonal species. However, the C−H stretching modes are isolated and virtually uncoupled, and the 3058.2, 3063.5, 3068.7, and 3073.1 cm⁻¹ trend is almost uniform with the number of F's replacing Cl on the Mo center. The C−H stretching frequency is expected to increase with s-character in the carbon hybrid orbital, and the s,p-character will depend on polarization of the C≡Mo triple bond by the halogen substituents.

The reaction proceeds following the mechanism suggested above with C−X insertion and two successive α-halogen transfer reactions to completely halogenate the metal center as shown in reaction 5. For chloroform, the methylidyne is 40 kcal/mol lower in energy than the methylidene complex, and this overall reaction is 147 kcal/mol exothermic; hence, the thermochemical driving force to form the carbyne is compelling. The increase on annealing suggests that the Mo and CHCl₃

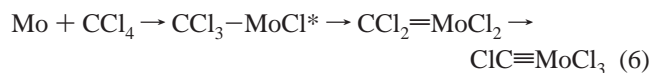reaction is spontaneous with ground-state metal atoms, which was the case for Li in the simple abstraction reaction.[41]

$$Mo + CHX_3 \rightarrow CHX_2-MoX^* \rightarrow CHX=MoX_2 \rightarrow$$
$$HC\equiv MoX_3 \quad (5)$$
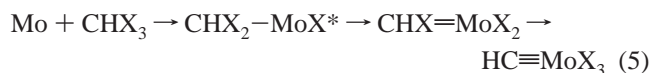
Mo + CX₄. The reactions of laser-ablated molybdenum atoms and tetrahalomethanes gave a product with very high C−F or C−Cl stretching frequencies. Infrared spectra for the reaction product of Mo with CCl₄ revealed new absorptions at 1259.6, 1253.3, and 443.6 cm⁻¹, which increased slightly on ultraviolet irradiation but not on annealing. With ¹³CCl₄, these bands shifted to 1215.6, 1209.4, and 442.5 cm⁻¹ (Figure 3). The reaction with CF₄ gave much weaker product absorptions at 1524.2, 682.3, and 664.3 cm⁻¹. The spectra in Figure S4 show that the product yield increases with the CF₃Cl and CF₂Cl₂ precursors, which gave strong new bands at 1523.8 and 1521.6 cm⁻¹ that shifted to 1476.6 and 1475.7 cm⁻¹ with the carbon-13-enriched precursors. These Freon reactions also provided new bands at 685.0 and 667.0, and at 670.6 and 473.9 cm⁻¹, respectively. Ultraviolet irradiation slightly increased the CF₄ and substantially increased the CF₃Cl and CF₂Cl₂ product absorptions.

The reaction with CCl₄ formed a single new metal-containing product with two strong absorptions at 1259.6 and 443.6 cm⁻¹, which correlate well with the two strongest absorptions calculated for the trigonal ClC≡MoCl₃ molecule. Table 6 compares the observed and calculated frequencies. First, the lower 1253.3 cm⁻¹ satellite is due to a matrix site splitting similar to that observed in the titanium system.[10] The major band at 1259.6 cm⁻¹ has a 1257.7 cm⁻¹ shoulder, which are appropriate for the vibration of ³⁵Cl and ³⁷Cl in natural abundance and verifies the participation of a single chlorine atom in this mode. Second, the weak carbon-12 band at 1259.6 cm⁻¹ in the 90% carbon-13 experiment with the strong 1215.6 cm⁻¹ carbon-13 coun-

(41) Carver, T. G.; Andrews, L. *J. Chem. Phys.* **1969**, *50*, 4235.

terpart demonstrates the presence of a single carbon atom in the product species. The antisymmetric Cl−C−Mo stretching mode is predicted at 1278.6 cm^{-1} with a 45.5 cm^{-1} carbon-13 shift, and our strong product band is observed at 1259.6 cm^{-1} with a 44.0 cm^{-1} shift. The high intensity and large carbon-13 shift for this mode are due in large part to the antisymmetric motion of carbon between the Cl and Mo centers. Correspondingly, the 1.9 cm^{-1} chlorine isotopic shift is less than the 8.8 cm^{-1} value expected for a diatomic C−Cl motion, but our B3LYP calculation predicts this to be 1.7 cm^{-1}, which is appropriate for the antisymmetric Cl−C−Mo stretching vibration.

The much weaker symmetric Cl−C−Mo stretching mode predicted at 453.7 cm^{-1} is not observed, but the degenerate antisymmetric Mo−Cl stretching mode calculated at 432.0 cm^{-1} with a 1.8 cm^{-1} carbon-13 shift is observed slightly higher at 443.6 cm^{-1} with a 1.1 cm^{-1} shift. The breadth of this band is appropriate for the contribution of natural Mo and Cl isotopes for the vibration of two or more chlorine atoms. This excellent correlation between calculated and observed frequencies and isotopic characteristics for the ClC≡MCl$_3$ molecule, which has a unique very high-frequency C−Cl stretching mode over 450 cm^{-1} higher than CCl$_4$ and other normal C−Cl single bond vibrations, confirms our assignment. Finally, this verifies that complete α-chlorine transfer reaction to saturate the Mo center has occurred and that the 162 kcal/mol exothermic overall reaction 6 has gone to completion. Again, energy released in the initial insertion reaction helps drive the successive α-chlorine transfers.

$$\text{Mo} + \text{CCl}_4 \rightarrow \text{CCl}_3\text{-MoCl}^* \rightarrow \text{CCl}_2{=}\text{MoCl}_2 \rightarrow$$
$$\text{ClC}{\equiv}\text{MoCl}_3 \quad (6)$$

Substantially weaker bands observed with CF$_4$ are assigned to the analogous vibrational modes, the antisymmetric F−C−Mo and Mo−F stretching modes, based on the calculated FC≡MoF$_3$ product frequencies as collected in Table 6. The symmetric F−C−Mo stretching mode is calculated at 619.0 cm^{-1} with practically no intensity. Reaction 6 for the fluorine system is exothermic by 114 kcal/mol, which reflects the stronger C−F bond energy. Analogous antisymmetric F−C−Mo stretching modes were observed at 1523.8 and 1521.6 cm^{-1} for the FC≡MoF$_2$Cl and FC≡MoFCl$_2$ products in the Freon-13 and 12 reactions. These latter bands exhibit the large carbon-13 shifts, 47.2 and 45.9 cm^{-1}, which are characteristic of these antisymmetric vibrational modes. In addition, two Mo−F stretching modes (685.0, 667.0 cm^{-1}) and one Mo−F and one Mo−Cl stretching mode (670.6, 473.9 cm^{-1}) are observed for these products. In the group 4 metal reactions with these chlorofluoromethanes, two structural isomers were observed with different numbers of chlorine and fluorine atoms transferred to the metal center.[11,12] In these experiments, the higher energy FCM form was favored on the deposition reaction with laser-ablated metal atoms, and subsequent UV photolysis reduced this in favor of the lower energy ClCM form. In the present case, it appears that only the 2 kcal/mol higher energy FC≡MoFCl$_2$ isomer is produced, and the same occurs for FC≡MoF$_2$Cl. Other possible lower oxidation state products in this system, the triplet ground-state methylidene complexes CF$_2$=MoCl$_2$, CFCl=MoFCl, and CCl$_2$=MoF$_2$, are 37, 42, and 42 kcal/mol higher in energy, and the quintet state analogues are 6, 9, and 12 kcal/mol higher still in energy, and these higher energy intermediate species are not observed.

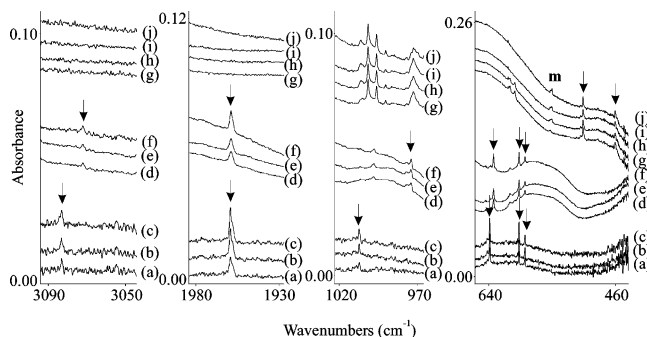**W + CH$_2$X$_2$.** The reaction of laser-ablated tungsten atoms and methylene chloride gave a set of weak product absorptions

Figure 7. Infrared spectra in selected regions for the W atom and CH$_2$Cl$_2$ reaction products in excess argon at 8 K. (a) W + 0.5% CH$_2$Cl$_2$ in argon co-deposited for 1 h. (b) After irradiation (λ > 220 nm). (c) After annealing to 30 K. (d) W + 0.5% ^{13}CH$_2$Cl$_2$ in argon co-deposited for 1 h. (e) After irradiation (λ > 220 nm). (f) After annealing to 30 K. (g) W + 0.5% CD$_2$Cl$_2$ in argon. (h) After irradiation (λ > 420 nm). (i) After irradiation (380−240 nm). (j) After annealing to 30 K. The label **m** denotes methylidene, arrows denote the methylidyne absorptions, and P denotes precursor bands.

at 3083.2, 1959.0, 1007.4, 638.9, 597.1, and 588.7 cm^{-1}, which decreased slightly on >420 nm irradiation, increased 10% on >290 nm and another 30% on >220 nm irradiation, and increased 20% on 30 K annealing and another 10% on final >220 nm irradiation. These new bands and their ^{13}CH$_2$Cl$_2$ and CD$_2$Cl$_2$ counterparts are shown in Figure 7, and the frequencies are listed in Table 7. They are comparable to the Mo counterparts except that the 1007.4 cm^{-1} band is sharp (full-width at half-maximum 0.9 cm^{-1}) as natural tungsten isotopes do not broaden the band like those for molybdenum.[37]

The deuterated sample also reveals a new 550.5 cm^{-1} band (labeled **m**) that increases on the initial >420 nm irradiation when the above band set decreases. Again, the CH$_2$Cl$_2$ counterpart probably falls under the strong precursor absorption. This band is due to a different product. Following the Mo/halomethane chemistry described above, and the related work on methyl halides,[16,18,20] the CD$_2$=WCl$_2$ molecule through which the reaction passes must be considered. Our calculations find the methylidene product CH$_2$=WCl$_2$ to be 6 kcal/mol higher in energy than the associated HC≡WHCl$_2$ methylidyne molecule, and the frequencies map those in Table 3 for the CH$_2$=MoCl$_2$ complex with some frequencies being slightly lower. The above 550.5 cm^{-1} band is analogous to the 542.2 cm^{-1} band assigned above to the CD$_2$ wagging mode of the CD$_2$=MoCl$_2$ methylidene where the CH$_2$ counterpart is masked by precursor absorption and the W−Cl stretching modes are too low to be observed here.

The above six-band set that increases on UV irradiation is assigned to the associated HC≡WHCl$_2$ methylidyne complex based on its relationship to the Mo counterparts and comparison with the calculated frequencies in Table 7. The C−H stretching frequency at 3083.2 cm^{-1} is just above that for the related HC≡WH$_2$Cl methylidyne complex at 3077.4 cm^{-1} [found by reanalysis of the spectrum].[20] The W−H stretching frequency at 1959.0 cm^{-1} may be compared to the 1926.2 and 1921.4 cm^{-1} values observed for HC≡WH$_2$Cl, and the frequencies for other functional groups are also comparable.[20] The final methylidyne complex is 7 kcal/mol more stable than the methylidene intermediate and 172 kcal/mol lower in energy than the reagents. Reaction 8 is photoreversible, but not nearly as
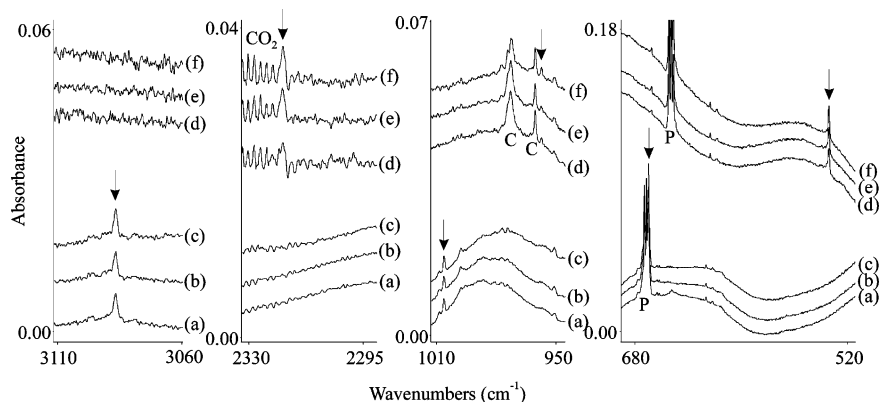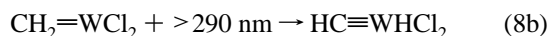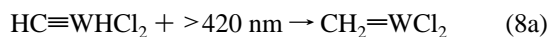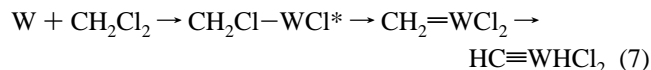
Figure 8. Infrared spectra in selected regions for the W atom and $CHCl_3$ reaction products in excess argon at 8 K. (a) W + 0.5% $CHCl_3$ in argon co-deposited for 1 h. (b) After irradiation (λ > 220 nm). (c) After annealing to 30 K. (d) Mo + 0.5% $CDCl_3$ in argon. (i) After irradiation (λ > 220 nm). (j) After annealing to 30 K. Arrows denote the methylidyne absorptions, and P denotes precursor bands.

Table 7. Observed and Calculated Fundamental Frequencies of the HC≡WHCl₂ Complex in the Ground ¹A′ Electronic State with Cₛ Structure[a]

approximate description	HC≡WHCl₂			H¹³C≡WHCl₂			DC≡WDCl₂		
	obs	calc	int	obs	calc	int	obs	calc	int
C−H str, a′	3083.2	3232.6	23	3072.1	3220.7	22	2317.3	2404.2	18
W−H str, a′	1959.0	2042.7	73	1959.0	2042.7	73	1409.9	1449.5	38
C≡W str, a′	1007.4	1052.4	11	974.4	1017.5	11	−[b]	1003.5	9
W−H def, a′		794.3	9		787.3	8		625.8	8
H−C−W def, a″	638.9	630.8	96	633.5	625.5	94	506.1	498.0	56
H−C−W def, a′	597.1	613.8	56	597.0	613.5	56	460.5	454.3	50
W−H def, a″	588.7	599.7	19	588.7	599.7	20		438.8	22
W−Cl str, a″		388.0	77		387.8	77		382.1	26
W−Cl str, a′		383.8	22		383.8	22		364.7	40

[a] Frequencies and intensities are in cm⁻¹ and km/mol. Three lower real frequencies are not listed. Observed in an argon matrix. Frequencies and intensities computed with B3LYP/6-311++G(2d,p) in the harmonic approximation using the SDD core potential and basis set are for W. The symmetry notations are based on the Cₛ structure. [b] Band covered by precursor.

much so as the dihydridomonochloro analogue, which has more hydrogen atoms available for transfer.[20]

$$W + CH_2Cl_2 \rightarrow CH_2Cl-WCl^* \rightarrow CH_2{=}WCl_2 \rightarrow$$
$$HC{\equiv}WHCl_2 \quad (7)$$

$$HC{\equiv}WHCl_2 + {>}420 \text{ nm} \rightarrow CH_2{=}WCl_2 \quad (8a)$$

$$CH_2{=}WCl_2 + {>}290 \text{ nm} \rightarrow HC{\equiv}WHCl_2 \quad (8b)$$

Our reaction of W with methylene fluoride produced weak new bands at 1978.6, 1015.6, 705.0, 675.3, and 601.3 cm⁻¹ upon >290 nm irradiation, which increased 3-fold on >220 nm photolysis. These bands relate to the above sets assigned to the HC≡WHCl₂ and HC≡MoHF₂ methylidyne complexes, and their assignment follows accordingly. The higher W−H frequency at 1978.6 cm⁻¹ follows the higher values of 1936.4 and 1930.4 cm⁻¹ for the HC≡WH₂Cl methylidyne.[18] In contrast to the methylene chloride case, the 8 kcal/mol higher energy CH₂= WF₂ complex was not observed in these experiments.

The CH₂=MX₂ complexes show no evidence of agostic distortion at the B3LYP computational level of theory, in contrast to the group 6 CH₂=MH₂ and CH₂=MHX methylidene complexes prepared from methane and methyl halides.[16−21] This observation is probably due in part to the 0.03 Å longer C=M bond lengths in the dihalide complexes.

W + CHX₃. Infrared spectra from the tungsten and chloroform reaction give bands similar to those found for Mo but displaced to 3087.7, 1006.4, 669.9, and 416.5 cm⁻¹, and again the 1006.4 cm⁻¹ band is sharp (0.9 cm⁻¹ bandwidth). The chloroform-carbon-13 product shifted to 3076.1, 973.5, 664.1, and 416.2 cm⁻¹. The chloroform-*d* product shifted to 2319.7,

957.2, 534.2, and 416.3 cm⁻¹, and these bands increased 10% on >290 and 220 nm irradiations and another 30% on annealing to 30 K. Representative spectra are shown in Figure 8 except for the lowest frequency bands (0.02 and 0.01 absorbance units, respectively). The observed frequencies are listed in Table 8 and compared to frequencies calculated for the HC≡WCl₃ methylidyne product, which is 52 kcal/mol lower in energy than the corresponding methylidene complex. The C−H stretching frequency is predicted 26 cm⁻¹ higher than for the Mo counterpart, and it is observed 29 cm⁻¹ higher. The B3LYP calculations do not fit as well for the C≡W and C≡Mo stretching modes as the C≡W mode is predicted 2 cm⁻¹ higher and observed 28 cm⁻¹ higher (shift between major metal isotopic positions). In addition, the W−Cl stretching mode is observed 18 cm⁻¹ higher than calculated, and the Mo−Cl stretching mode is observed 14 cm⁻¹ higher than calculated. However, both H−C−M deformation modes are observed within 2 cm⁻¹ of the calculated values. Overall, the correlation between calculated and observed frequencies for the HC≡MCl₃ methylidyne complexes is very good and confirms our assignments.

The fluoroform reaction gives weaker product bands at 3103.2, 683.2, 677.6, and 651.4 cm⁻¹, which increase 100% over the course of >290 nm, >220 nm irradiation, 30 K annealing, and a second >220 nm irradiation. These bands are 1, 2, 4, and 7 × 10⁻³ absorbance units, respectively, which matches very well the predicted infrared intensities of the computed frequencies in Table 8. As mentioned above, the W−F stretching frequencies are computed slightly low, and in this case the most intense degenerate H−C−W deformation mode

Table 8. Observed and Calculated Fundamental Frequencies of HC≡WCl₃ and HC≡WF₃ Complexes in the Ground ¹A₁ Electronic State with C₃ᵥ Structure[a]

approximate description	HC≡WCl₃			H¹³C≡WCl₃			DC≡WCl₃			HC≡WF₃		
	obs	calc	int	obs	calc	int	obs	calc	int	obs[b]	calc	int
C–H str, a₁	3087.7	3238.5	30	3076.1	3226.6	29	2319.7	2408.5	22	3103.2	3250.0	35
HC≡W str, a₁	1006.4	1053.5	9	973.5	1018.5	9	957.2	1004.7	7		1073.0	19
H–C–W def, e	669.9	670.9	82 × 2	664.1	664.7	81 × 2	534.2	533.7	48 × 2	651.4	646.0	154 × 2
W–X str, e	416.4	398.7	74 × 2	416.2	398.6	75 × 2	416.3	398.5	72 × 2	677.6	660.7	73 × 2
W–X str, a₁		386.5	10		386.5	10		386.5	10	683.3	662.6	65
C–W–X def, e		238.8	3 × 2		233.2	2 × 2		215.7	3 × 2		289.2	1 × 2
W–X₃ umb, a₁		133.1	0		133.0	0	133.0		0		216.4	7
W–X₂ bend, e		98.5	0		98.5	0	98.5		0		158.4	6 × 2

[a] Frequencies and intensities are in cm⁻¹ and km/mol. Observed in an argon matrix. Frequencies and intensities computed with B3LYP/6-311++G(2d,p) in the harmonic approximation using the SDD core potential and basis set for W. The symmetry notations are based on the C₃ᵥ structure. [b] Relative intensities 1, 2, 4, 7 × 10⁻³ absorbance units, respectively, in order of decreasing frequency.

Table 9. Comparison of Bond Lengths and Characteristic Frequencies for Related H–C≡W Compounds

d, Å or fr, cm⁻¹	H–C≡W[a]	H–C≡WH₃[b]	H–C≡WCl₃[c]	H–C≡W(PMe₃)₄Cl[d]
d(C–H)	1.0765	1.081	1.081	1.092–1.093
d(C≡W)	1.7367	1.742	1.751	1.79–1.80
fr(C–H)		3076	3087	2994, 2978
fr(HC≡W)	1006	1003	1006	909
fr(H–C–W)	660	727	670	788, 755
fr(C–D)			2320	2244, 2234
fr(DC≡W)	953	953	957	871
fr(D–C–W)	501	571	534	642, 611

[a] Gas-phase measurements, ref 9. [b] B3LYP calculated bond lengths and argon matrix frequencies, ref 19. The C–H stretching frequency was too weak to observe, but the 3076 cm⁻¹ value is extrapolated from that for the related HC≡WH₂Cl methylidyne complex at 3077 cm⁻¹. [c] B3LYP calculated bond lengths and argon matrix frequencies, this work. [d] Microcrystalline sample, ref 7.

is computed about 5 cm⁻¹ below the observed value. Overall, the correlation between calculated and observed frequencies for this demanding HC≡WF₃ subject molecule is gratifying.

The tungsten reaction with chloroform is overall even more exothermic, 220 kcal/mol, than the molybdenum counterpart, and the methylidene intermediate is 52 kcal/mol higher in energy than the final methylidyne product, and as before the fluoroform reaction is less exothermic (211 kcal/mol). These B3LYP energy calculations underscore the stability of the final very stable methylidyne product.

$$W + CHCl_3 \rightarrow CHCl_2–WCl^* \rightarrow CHCl=WCl_2 \rightarrow$$
$$HC≡WCl_3 \quad (9)$$
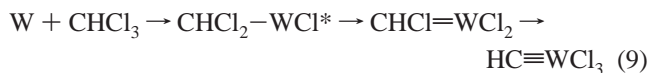
W + CX₄. Spectra from the reaction products of laser-ablated tungsten atoms and tetrahalomethanes are similar to those for molybdenum, and the spectra are compared in Figures 3 and S6. The CCl₄ product absorptions are higher at 1292.8, 1287.3 cm⁻¹ and lower at 416.0 cm⁻¹, and the carbon-13 shifts are 46.2, 46.1, and 0.5 cm⁻¹, respectively. The 1287.3 cm⁻¹ component is a matrix site splitting, but a partially resolved shoulder on the major 1292.8 cm⁻¹ band at 1291.1 cm⁻¹ forms precisely the 3/1 pattern expected for natural abundance chlorine isotopes and the vibration of a single chlorine atom. The larger carbon-13 and smaller chlorine-37 shifts, as compared to the molybdenum counterparts, are due to the involvement of a heavier metal and further characterize this antisymmetric Cl–C–M vibration. Our B3LYP calculation predicts the carbon and chlorine isotopic shifts as 47.3 and 1.7 cm⁻¹, and we observe them as 46.2 and 1.7 cm⁻¹. The 416.0 cm⁻¹ band is due to the antisymmetric W–Cl stretching vibration as shown in Table S9.

The CF₄ product absorptions are higher such that the upper band is covered by precursor and the lower bands are at 676.1 and 671.2 cm⁻¹. With the CF₃Cl and CF₂Cl₂ reagents, strong new bands were observed at 1541.2 and 1538.2 cm⁻¹, and the former shifted to 1492.9 cm⁻¹ with the carbon-13-enriched

precursor. These high-frequency bands are due to C–F stretching modes in FC≡WF₂Cl and FC≡WFCl₂, respectively. These Freon precursors also provided new bands at 654.2 and 638.9, and at 711.8, 675.4, and 585.7 cm⁻¹, respectively. Ultraviolet irradiation substantially increased the product absorptions.

Reaction 10 for tungsten is even more exothermic, 234 kcal/mol, than the molybdenum counterpart, but the W reaction with CF₄ is less exothermic, 189 kcal/mol, all calculated at the B3LYP level of theory.

$$W + CCl_4 \rightarrow CCl_3–WCl^* \rightarrow CCl_2=WCl_2 \rightarrow$$
$$ClC≡WCl_3 \quad (10)$$
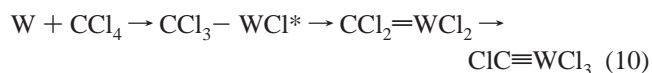
C–H, C≡M, and X–C–M Stretching Frequencies. After the observation and characterization of these new trigonal HC≡MX₃ and XC≡WX₃ methylidyne molecules, the most interesting and informative measurable parameters are the C–H, C≡M, and X–C–M stretching frequencies. The C–H stretching frequencies in the HC≡MoF$_n$Cl$_{3-n}$ (n = 0, 1, 2, 3) series increase from 3058.2, 3063.5, 3068.7, to 3073.1 cm⁻¹ with the number of F's replacing Cl on the Mo center. This is opposite the trend in the CHCl₃ (3053.4 cm⁻¹) and CHF₃ (3043.5 cm⁻¹) precursors. These C–H stretching frequencies are higher than normal alkane values (3028.5 cm⁻¹ for methane in solid argon), which suggests an adjacent multiple carbon–metal bond to provide higher s-character to the C–H bond,[4,42] although acetylene (3288.9 cm⁻¹ in solid argon) and methylacetylene (3322.8 cm⁻¹ in solid argon)[43] are considerably higher. Table S10 shows that the s-character from NBO analysis[26,30] increases in the above series with the increase in C–H stretching frequencies and decrease in computed C–H bond length, although this decrease is only 0.0009 Å. The calculated frequencies, of course, and the infrared intensities follow the same trend. The natural charges show that the C≡M bond

(42) Pavia, D. L.; Lampman, G. M.; George, S. K. *Introduction to Spectroscopy*, 3rd ed.; Brooks Cole: New York, 2000.

(43) Andrews, L.; Johnson, G. L. *J. Phys. Chem. A* **1982**, *86*, 3380.
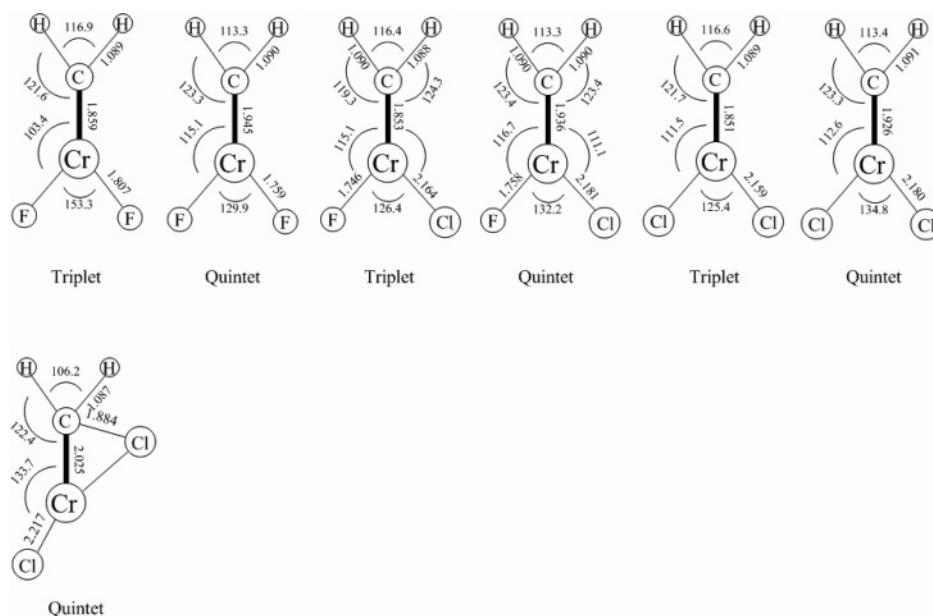
Figure 9. Structures of the $CH_2=CrX_2$, CH_2-CrX_2, and $CH_2Cl-CrCl$ complexes optimized at the level of B3LYP/6-311++G(2d,p)/SDD. The bond lengths and angles are in Å and deg. Spin multiplicities are given underneath.
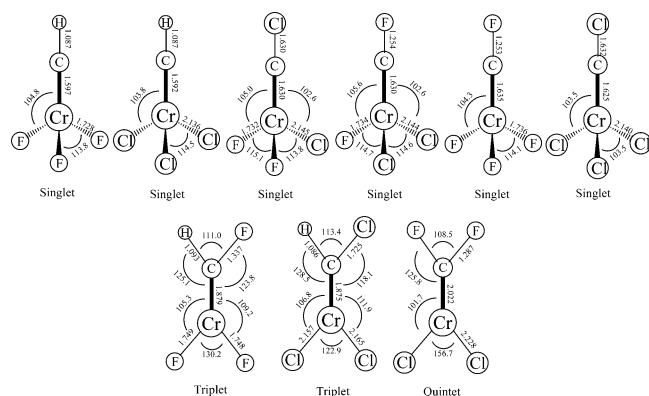

Figure 10. Structures of the $HC≡CrX_3$, $XC≡CrX_3$, $CHX=CrX_2$, and $CF_2=CCl_2$ complexes optimized at the level of B3LYP/6-311++G(2d,p)/SDD. The bond lengths and angles are in Å and deg. Spin multiplicities are given underneath.
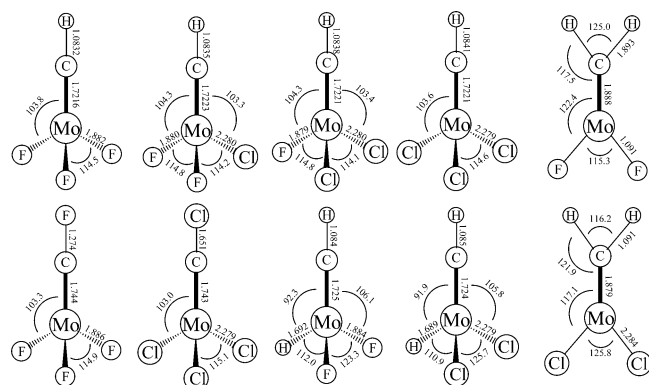

Figure 11. The structures of $CH_2=MoX_2$, $HC≡MoX_3$, and $XC≡MoX_3$ molecules optimized using B3LYP/6-311++G(2d,p)/SDD methods. The bond lengths and angles are in Å and deg.

Figure 12. The structures of $CH_2=WX_2$, $HC≡WX_3$, and $XC≡WX_3$ molecules optimized using B3LYP/6-311++G(2d,p)/SDD methods. The bond lengths and angles are in Å and deg.

polarization increases with F substitution, and the C−H stretching infrared intensity follows. The same rationale applies to the $HC≡MoF_nH_{3-n}$ ($n = 0, 1, 2, 3$) series of methylidynes[16,17] where the calculated C−H frequency and infrared intensity increase with fluorine substitution, and this mode has been observed only for the most intense $n = 3$ member of the series.
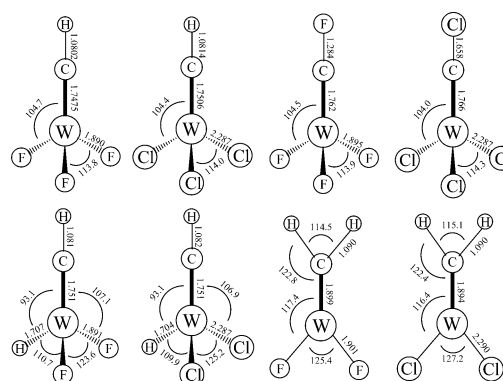
However, re-examination of the $HC≡WH_2F$ spectrum[18] reveals the weak C−H stretching mode at 3081.6 cm^{-1}, and likewise for the related $HC≡WH_2Cl$ methylidyne complex[20] at 3077.4 cm^{-1} and the bromine analogue at 3076.0 cm^{-1}. Our calculation for $HC≡WHCl_2$ predicted the C−H stretching mode 5 cm^{-1} higher than for $HC≡WH_2F$, and we observed this mode 2 cm^{-1} higher, which is in very good agreement. We have now observed C−H stretching modes for the last three members of the $HC≡WCl_nH_{3-n}$ ($n = 0, 1, 2, 3$) series of methylidynes (3077.4, 3083.2, and 3087.0 cm^{-1}). Our calculations show that the all-hydrogen $n = 0$ species, which we were unable to observe due to low reaction yield, extrapolates 1 cm^{-1} lower than $HC≡WH_2Cl$ at 3077.4 cm^{-1}, and they allow us to evaluate this mode for $HC≡WH_3$ as 3076 cm^{-1} (Table 9).

The computed s-character is highest in the $HC≡MoF_3$ and $HC≡WF_3$ molecules (48.5%, 48.4%, respectively), and the C−H stretching frequencies are the highest we observe (3073, 3103 cm^{-1}). Our calculations predict the C−H stretching mode for the tungsten methylidyne to be 29 cm^{-1} higher than that for the molybdenum analogue, and we observe it to be 30 cm^{-1} higher (Table S10).

Notice that the C≡M stretching frequencies also follow the same increasing trend with fluorine substitution. The π bonds show no variation in hybridization in the series, but a small

Table 10. Comparison of Characteristic Frequencies for Related HC≡MCl₃ Methylidyne Molecules in Solid Argon

mode	HC≡CrCl₃	DC≡CrCl₃	HC≡MoCl₃	DC≡MoCl₃	HC≡WCl₃	DC≡WCl₃
C—H str	3038.5	covered[a]	3058.2	2296.2	3087.7	2319.7
C≡M str	not obs	not obs	978.1	932.4	1006.4	967.2
H—C—M def	637.8	533.7	658.9	533.4	670.0	534.2
C—X₃ str	488.9	477.6	438.7	436.4	416.5	416.3

[a] Covered by precursor absorption.

decrease in carbon 2s character is accompanied by a large increase in Mo 5s character in the carbon—molybdenum σ bond.

The C—H stretching frequency of the related HC≡MoHCl₂ methylidyne is 3 cm⁻¹ lower than that for HC≡MoCl₃, and the s-character is slightly, 0.7%, lower. The same consistency is observed within the tungsten pair HC≡WCl₃ and HC≡WHCl₂, where the latter C—H frequency is 4 cm⁻¹ lower and the s-character 0.5% lower. However, the comparison between Mo and W is not consistent as the C—H frequency is higher for the W species but the s-character lower, although the differences are small. We believe that this is due to an imperfect application of the SDD pseudopotential and basis for this particular comparison.

The very high C—X stretching frequencies and large carbon-13 shifts observed for the XC≡MX₃ methylidynes indicate that these are in fact due to antisymmetric stretching of the C atom between the halogen and metal masses. The carbon-13 shift for a diatomic C—Cl stretching mode at the 1259.6 cm⁻¹ frequency observed for ClC≡MoCl₃ would be 36.9 cm⁻¹, and the observed carbon-13 shift is 44.0 cm⁻¹. The pure antisymmetric stretch of a linear Cl—C—Cl linkage would shift 42.3 cm⁻¹, and our B3LYP calculation for this Cl—C—Mo mode finds 45.5 cm⁻¹ for the antisymmetric motion of C between Cl and Mo. This point is substantiated by comparing the higher 1292.6 cm⁻¹ frequency for ClC≡WCl₃ and the larger 46.2 cm⁻¹ carbon-13 shift (3.57% for C moving against W as compared to 3.49% with Mo and to 3.35% with Cr). Hence, the very high C—X stretching frequency with such a very large carbon-13 shift is also diagnostic of the unique bonding in the XC≡MX₃ methylidyne molecules.

A final comparison of the new HC≡WCl₃ molecule is of particular interest because the gaseous HC≡W species, the simple hydrogen derivative HC≡WH₃, and the thoroughly investigated microcrystalline HC≡W(PMe₃)₄Cl complex[7,9,19] provide a wide range of tungsten methylidyne compounds for comparison of methylidyne frequencies and bond lengths. The photophysics of these latter complexes is tunable by changing substituents[44] like the C—H stretching frequency described above. Important parameters are collected in Table 9. First, the bond lengths are measured to four decimal places for the gaseous HC≡W species,[9] and these are all slightly shorter than our B3LYP calculated values for the methylidynes and estimated values for the solid-state complex.[7] The frequencies measured for HC≡W have to be taken as benchmarks, and the HC≡W mode (1006 cm⁻¹) and its DC≡W (953 cm⁻¹) counterpart show that there is coupling with H(D). Our methylidyne complex values, 1003(953) and 1006(957) cm⁻¹, are extremely close. However, the microcrystalline complex frequencies are 97 and 82 cm⁻¹ lower, and other methylidyne complex values are in the 1300—1400 cm⁻¹ range,[5] which demonstrates considerable coupling to other modes in these organometallic complexes. The H—C—W and D—C—W deformation modes for the gaseous species are 660 and 501 cm⁻¹. As the data in Table 9 show, these modes increase with molecular complexity including ligands and even split in the solid state. In the case of our HC≡

WCl₃ complex, the W—Cl stretching modes are too low (416 cm⁻¹ and lower) to perturb significantly the important diagnostic HC≡W modes, and accordingly our HC≡W group frequencies approach the gaseous values. Finally, and perhaps the most interesting, is the C—H stretching mode, which is also split in the solid state and about 100 cm⁻¹ lower than in the HC≡WCl₃ methylidyne molecule in solid argon. We suggest that our simple methylidyne molecule is more representative of the methylidyne C—H stretching modes, as it is only encumbered by argon matrix and not ligand and solid-state effects.

Bonding and Structure Comparisons. Several comparisons within the important group 6 transition metal family methylidene and methylidyne molecules are of interest. First, consider the calculated structures illustrated in Figures 9—12. The C≡Cr triple bonds are all computed to be in the 1.592—1.635 Å range, which is slightly shorter than the 1.735—1.745 Å values measured by X-ray for heavily ligated chromium carbyne complexes.[3a,14] This is outside of the error range of our B3LYP calculation, and it shows that the ligated complex triple bonds are longer than the C≡Cr triple bonds prepared in these simple matrix isolated methylidyne molecules. Second, notice that fluorine substitution for chlorine on the chromium center very slightly elongates the double and triple carbon—chromium bonds. This is due to contraction of the metal 3d orbitals by the inductive effect of fluorine, which makes them less effective in forming π bonds to carbon. Third, notice that there is no evidence for agostic distortion in the methylidene complexes, which have C₂ᵥ computed structures. This is in contrast to the monohalo methylidene complexes of Mo and W, which are agostic.[16-21]

Table 10 compares the frequencies for the series of the simple methylidyne molecules HC≡MCl₃ for M = Cr, Mo, and W. The C—H stretching frequency increases with metal size as the calculated C—H length decreases from 1.0874 to 1.0841 to 1.0814 Å. The s-character in the carbon hybrid orbital increases from 44.3% for the Cr methylidyne to 46.3% for the Mo and 46.0% for the W species. (We are unsure why the W is not higher than the Mo value, but we are using SDD pseudopotential and basis sets developed from other atomic and molecular data.[29] We do note that the values for Mo and W are similar, and Cr is lower than both.) We also point out that the natural charges on C and Cr (0.18, 0.28) indicate very little bond polarity, in marked contrast to the Mo and the even more polar W examples. This is also accompanied by an increase in the H—C—M deformation frequency. The H—C—M/D—C—M frequency ratio also increases slightly, 1.195, 1.235, 1.254, which is a measure of harmonic character in the vibrational potential function. The H/D ratio for the analogous mode in HC≡CrF₃ is nearly the same, 1.199, so this quantity is metal dependent. Unfortunately, the C≡Cr stretching mode is calculated to be too weak to observe, but in the same region as the C≡Mo and C≡W stretching modes, which were observed with natural metal isotopic profiles.

The increasing stability of the heavier metal methylidynes is underscored by the reaction exothermicities collected in Table S11. Notice that the chromium product formation reaction

(44) Da Re, R. E.; Hopkins, M. D. *Coord. Chem. Rev.* **2005**, *249*, 1396.

exothermicities are about one-half or less than those for molybdenum, which are substantially less than the values for tungsten. The fluoride reactions are less exothermic due to the stronger C−F bond energy as compared to C−Cl. Furthermore, the Cr and Freon reactions give predominantly methylidene with little methylidyne product. This trend is an extension of the energy profile presented for the group 6 metal and CH_3F reaction products, which showed that chromium methylidenes and methylidynes are higher energy species.[18]

It is also of interest to compare the carbon-13 and chlorine-37 isotopic shifts in the antisymmetric Cl−C−M stretching mode for the $ClC≡MCl_3$ molecules observed at 1230.6, 1259.6, and 1292.8 cm^{-1}, respectively, for Cr, Mo, and W. The isotopic shifts are expressed as % of the frequency for C and Cl, respectively, as follows: Cr (3.35, 0.20), Mo (3.49, 0.15), and W (3.57, 0.13). In this antisymmetric stretching mode, carbon is moving most, and C will move more against the heavier W resulting in less motion for the Cl atom.

Conclusions

Reactions of laser-ablated Cr, Mo, and W atoms with di-, tri-, and tetrahalomethanes have produced a series of new methylidene $CH_2=MX_2$ and methylidyne molecules $HC≡MHX_2$, $HC≡MX_3$, and $XC≡MX_3$ (X = F, Cl). Matrix-isolation infrared spectra and quasi-relativistic density functional methods have been used to identify the new products formed by highly exothermic metal atom reactions in these experiments. Symmetrical trigonal structures were computed for the latter methylidyne molecules. Bonding analyses were performed using natural bond orbitals, and the C−H stretching frequencies were shown to increase with increasing s-character in the carbon hybrid orbitals in the $HC≡MoF_nCl_{3-n}$ (n = 0, 1, 2, 3) series. Comparisons with the gaseous HC≡W species, the simple hydrogen derivative $HC≡WH_3$, the new $HC≡WCl_3$ molecule, and the microcrystalline $HC≡W(PMe_3)_4Cl$ complex[7,9,19] underscore the close chemical relationship among these species

and show the effect of substituents and the solid state on the important diagnostic methylidyne vibrational frequencies.

In contrast to the group 6 $CH_2=MH_2$ and $CH_2=MHX$ methylidene complexes prepared from methane and methyl halides,[16–21] the $CH_2=MX_2$ complexes show no evidence of agostic distortion at the B3LYP computational level of theory. This may be in part due to the 0.03 Å longer C=M bond lengths in the dihalide complexes.

The Cr reactions with methylene halides gave triplet $CH_2=CrCl_2$ and $CH_2=CrFCl$ or quintet $CH_2−CrF_2$ methylidene complexes as major products, in contrast to previous investigations with methane and methyl halides, which formed only quintet $CH_3−CrX$ insertion products.[18–21] The observation of methylidynes in Cr reactions with haloforms and carbon tetrahalides highlights the importance of halogen atoms as α-transfer reagents to increase the reaction exothermicity and thus to favor the formation of the higher oxidation state methylidyne molecules. The C−H stretching mode at 3038.5 cm^{-1} and the 44.3% carbon 2s character for $HC≡CrCl_3$ are the lowest we have observed for a group 6 metal. The present simple methylidyne complex C≡Cr bond lengths calculated in the 1.59−1.63 Å range demonstrate the effect of bulky substituents and the solid state on these fundamental molecular parameters,[3a,14] and our simple complexes should be used as the benchmark for comparison of chromium methylidyne physical constants.

Note Added after ASAP Publication. Table 2 contained errors in the version published ASAP November 7, 2007; the corrected version published ASAP November 12, 2007.

Supporting Information Available: Tables of calculated frequencies and figures of matrix infrared spectra. This material is available free of charge via the Internet at http://pubs.acs.org.

OM700689E